DOI: 10.1002/ejic.201100479

Redox Chemistry and Group 10 Metal Complexes of Aromatic Compounds with Bulky Bicyclic Guanidino Groups

Ute Wild,[a] Elisabeth Kaifer,[a] and Hans-Jörg Himmel*[a]

Keywords: Redox chemistry / Nickel / Palladium / Platinum / Guanidine / Coordination compounds

The reaction between activated bicyclic tetramethylbisurea and 1,2-diaminobenzene or 1,2,4,5-tetraaminobenzene affords new aromatic compounds functionalized with bicyclic guanidino groups. Protonation and redox reactions are carried out to obtain information about the chemical properties of these new guanidines. They are used as chelating ligands in mononuclear and dinuclear group 10 metal (Ni, Pd, and Pt) complexes, which could be interesting for catalytic applications. Initial experiments with a Ni complex showed a moderate activity in olefin oligomerization yielding mostly C_6 hydrocarbons.

Introduction

Bisimines are interesting ligands in the design of highly active homogeneous catalysts. For example, Ni and Pd complexes with sterically demanding bisimine ligands, such as ArN=C(R)C(R)=NAr and 2,6-(ArN=CR)$_2$C$_5$H$_3$N (R = H or alkyl, Ar = aryl, Scheme 1), have been widely applied in catalytic olefin polymerization, and are especially attractive for the polymerization of functionalized olefins.[1–3] The properties of the Ar substituents, in particular their steric requirements, generally control the molecular weight of the oligomers or polymeric chains.

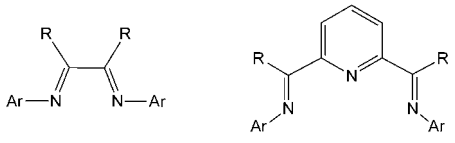

Scheme 1.

Guanidines, which are special imines, and guanidinates exhibit a rich coordination chemistry, which is of interest for a variety of applications.[4–11] 1,2-Bis(tetramethylguanidino)benzene (btmgb),[12,13] and 1,2-bis(*N*,*N*′-dimethylethyleneguanidino)benzene (bdmegb),[14,15] shown in Scheme 2, are examples of bisguanidines that can coordinate to transition metal centers through their imino N atoms, similar to other bisimine ligands. Indeed a number of mononuclear metal complexes of these two ligands have already been studied.[16,17] If further guanidino groups are introduced in positions four and five of the benzene ring, the redox-active, relatively strong electron donors 1,2,4,5-tetrakis(tetramethylguanidino)benzene (ttmgb) and 1,2,4,5-tetrakis(*N*,*N*′-dimethylethyleneguanidino)benzene (tdmegb) are obtained (Scheme 2), which can coordinate two metal centers.[18–24] Although oxidation, for example of ttmgb, generally leads directly to the dications (presumably due to ion pairing), the monocationic radical [ttmgb]$^{\cdot+}$ has been stabilized in a dinuclear Cu^{II} complex.[22]

Herein we report the synthesis of two new guanidine ligands **1** and **2** (Scheme 2), which are the products of the reaction between activated bicyclic tetramethylbisurea (tetramethylglycoluril) and 1,2-diaminobenzene or 1,2,4,5-tetraaminobenzene. In comparison to the other guanidine ligands shown in Scheme 2, the steric demand of the guanidino groups is larger due to the curved architecture of the bicyclic ring system (the H atoms at the ring junction are *cis* to each other). This could make these two bisimine ligands potentially attractive for catalytic applications.

Results and Discussion

Synthesis and Characterization of 1 and 2

The new guanidine ligands were synthesized by the reaction between bicyclic tetramethylbisurea (tetramethylglycoluril) and 1,2-diaminobenzene or 1,2,4,5-tetraaminobenzene. Bicyclic bisurea (bbu, glycoluril) and its derivatives are well known, especially for their self-assembly and condensation reactions with formaldehydes to give macrocycles.[25–29] The resulting macrocycles can be used, for example, as receptors, for the incorporation of organic guests or transition metal complexes, and for chiral recognition.[30] The three-step synthesis of **1** started with bicyclic tetramethylbisurea (other names 1,3,4,6-tetramethyltetrahydro-

[a] Anorganisch-Chemisches Institut, Ruprecht-Karls-Universität Heidelberg,
Im Neuenheimer Feld 270, 69120 Heidelberg, Germany
Fax: +49-6221-545707
E-mail: hans-jorg.himmel@aci.uni-heidelberg.de

Supporting information for this article is available on the WWW under http://dx.doi.org/10.1002/ejic.201100479.

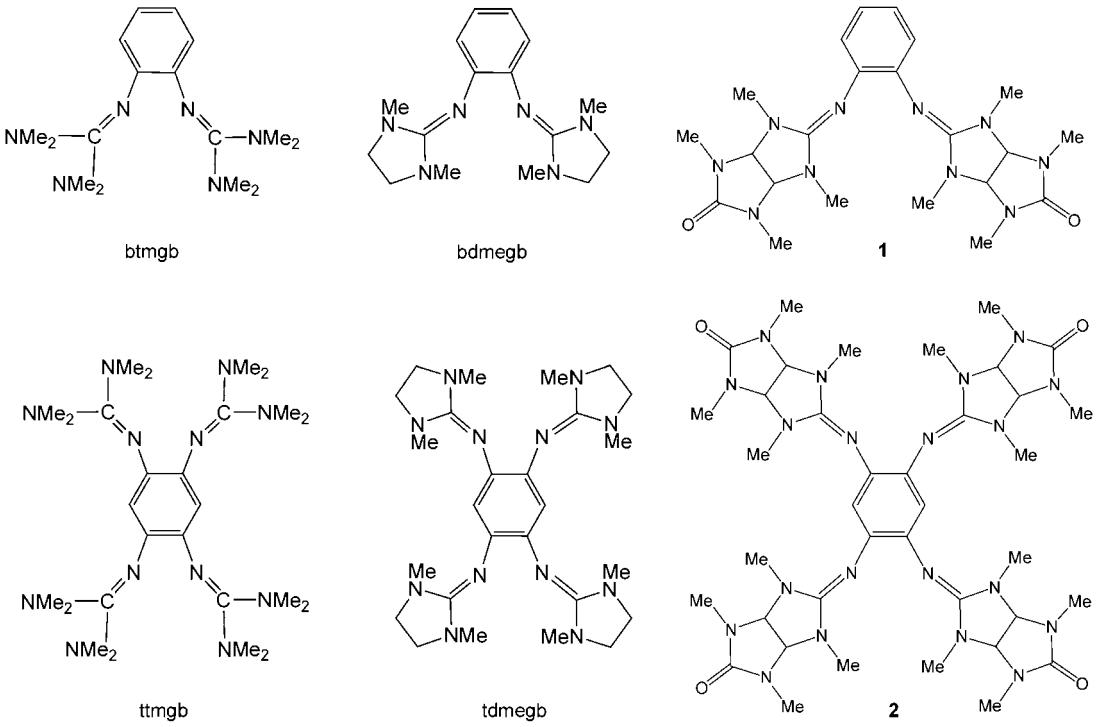

Scheme 2.

imidazo[4,5-*d*]imidazole-5-one or tetramethylglycoluril, Scheme 3), which is also known by the name "mebikar" as a polyfunctional pharmaceutical.[31–33]

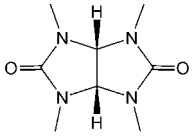

Scheme 3.

This molecule can be prepared from a condensation reaction between glyoxal and *N*,*N*′-dimethylurea, $(MeNH)_2CO$. In the second step, this bisurea was activated with oxalyl chloride to give the Vilsmeier salt; see Equation (1).

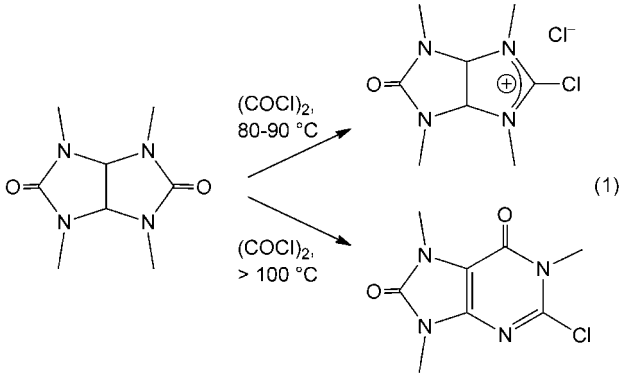

The temperature of the reaction mixture during this step was kept below 100 °C, as another product is formed at higher temperatures. The high-temperature product was crystallized from CH_3CN solutions, and featured fused five- and six-membered rings [see Equation (1) and the Supporting Information]. In the third step the activated bisurea was reacted with 1,2-diaminobenzene. Crystals of **1** suitable for XRD analysis were obtained from CH_3CN solutions, and Figure 1 illustrates its molecular structure. As anticipated, the two substituents adopt a *cis* configuration at the ring junction. The dihedral angle formed by the mean planes of the five-membered rings is 121.2°, which compares well with a corresponding angle in 2,8-dimethyl-bicyclic bisurea of 121.4(1)°.[34] At 129.13(14) pm, the lengths of the two imino N=C bonds of **1** fall into characteristic regions. For comparison, in the related bisguanidines btmgb and bdmegb the imino C=N bond lengths measure 129.1(3)/130.1(3)[13] and 128.0/128.4 pm,[15] respectively. The N···N

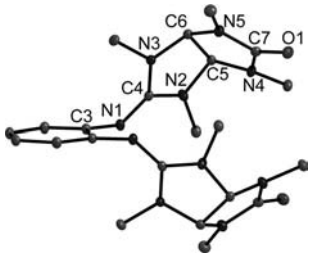

Figure 1.Molecular structure of **1** (hydrogen atoms omitted for clarity). Vibrational ellipsoids are drawn at 50% probability. Selected structural parameters (bond lengths in pm, bond angles in °): N1–C3 141.74(13), N1–C4 129.13(14), N2–C4 137.56(14), N2–C5 144.23(14), N3–C4 137.69(14), N3–C6 145.55(14), N4–C5 144.94(14), N4–C7 136.63(14), N5–C6 144.50(14), N5–C7 135.90(14), O1–C7 123.47(14), C3–C3′ 141.2(2), C5–C6 154.55(15), C3–N1–C4 123.18(9), N2–C4–N3 108.29(9), N2–C5–N4 115.39(9), N3–C6–N5 104.16(9), N4–C7–N5 108.84(9).

separation between the two imino N atoms of the guanidino groups in **1** [295.3(5) pm] is larger by ca. 10 pm than that of btmgb [285.8(2) pm],[13] presumably due to the increased steric demand of the bicyclic guanidino groups in **1**.

Reaction of activated bicyclic tetramethylbisurea with 1,2,4,5-tetraaminobenzene afforded **2**, which was crystallized from a saturated CH_3CN solution. Figure 2 shows its molecular structure. The interguanidino imino N···N separation of 297.5(4) in **2** compares well with that of 295.3(5) pm in **1**. The N=C double bond lengths measures 128.7(2)/128.8(2) pm. Figure 3 displays the UV/Vis spectra of **1** and **2**. In the spectrum recorded for **1**, bands at 225 (with a shoulder near 234 nm), 267, and 306 nm are observed. The spectrum for **2** also contains three bands, which

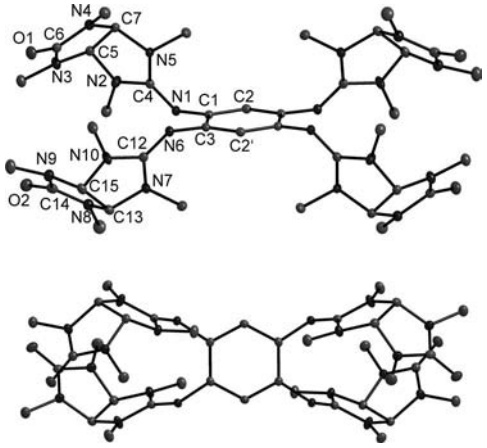

Figure 2. Molecular structure of **2** (hydrogen atoms omitted for clarity). Vibrational ellipsoids are drawn at 50% probability. Selected structural parameters (bond lengths in pm, bond angles in °): N1–C1 141.8(2), N1–C4 128.7(2), N2–C4 137.1(2), N2–C5 143.2(2), N3–C5 145.4(2), N3–C6 136.2(2), N4–C6 136.0(2), N4–C7 144.9(2), N5–C4 138.4(2), N5–C7 145.6(2), N6–C3 141.62(19), N6–C12 128.8(2), N7–C12 137.2(2), N7–C13 145.0(2), N8–C13 144.8(2), N8–C14 136.3(2), N9–C14 136.5(2), N9–C15 144.9(2), N10-C12 137.0(2), N10-C15 144.1(2), C6–O1 123.70(19), C14–O2 123.3(2), C1–C2 139.5(2), C1–C3 141.0(2), C2′–C3 139.2(2), C5–C7 155.1(2), C13–C15 154.4(2), C1–N1–C4 121.06(13), N2–C4–N5 108.37(14), N3–C6–N4 109.09(14), C3–N6–C12 122.03(13), N7–C12–N10 107.96(14), N8–C14–N9 108.86(15).

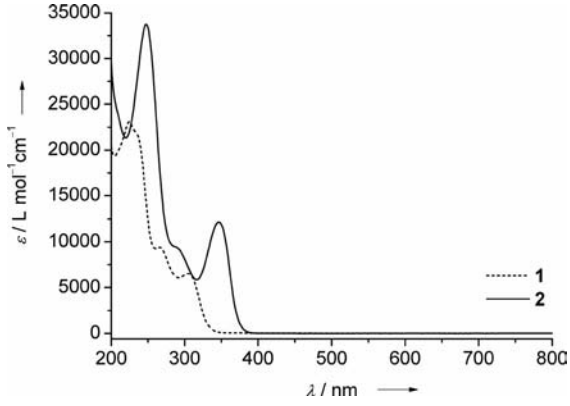

Figure 3. UV/Vis spectra of **1** and **2** in CH_3CN.

are, however, redshifted with respect to **1** (247, 290, and 347 nm). For comparison, the spectrum of btmgb contains a single band at 292 nm.[18]

Protonation Experiments

Guanidino-functionalized naphthalene species such as 1,8-bis(tetramethylguanidino)naphthalene[35] and 1,4,5,8-tetrakis(tetramethylguanidino)naphthalene[21,36] have been shown to be proton sponges. Hence the monoprotonated form of these species features the proton in an unsymmetric bridging position between both imino N atoms. Protonation experiments with **1** and **2** were carried out to probe if they behave as proton sponges. The reaction of **1** with HCl yielded $[\mathbf{1}H_2]Cl_2{\cdot}H_2O$. The structure derived from XRD analysis is depicted in Figure 4. As anticipated, protonation occurred exclusively at the two imino N atoms. The N=C bond lengths in $[\mathbf{1}H_2]^{2+}$ are 133.3(3)/133.3(4) pm, and the interguanidino distance (imino N···N separation) is 298.1(4) pm. As illustrated in Figure 4 (b), 1D networks were formed in the crystalline state, in which the protonated ligand units are connected by hydrogen bonding interactions involving chloride ions and water molecules. In CD_3CN solution, the N–H protons were observed at δ = 12.01 ppm in the ^1H NMR spectra. For comparison, the corresponding signal of $[btmgbH_2]^{2+}$ was found at δ = 11.24 ppm (also in CD_3CN).[13]

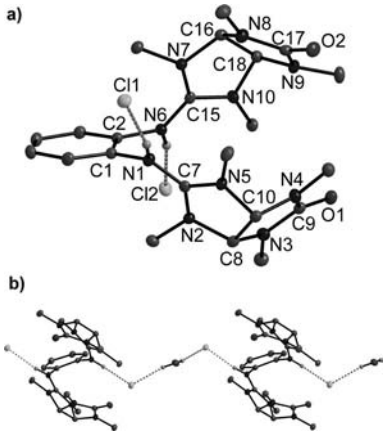

Figure 4. a) Molecular structure of $(\mathbf{1}H_2)Cl_2{\cdot}H_2O$ (hydrogen atoms omitted for clarity). Vibrational ellipsoids are drawn at the 50% probability level. Selected structural parameters (bond lengths in pm, bond angles in °): N1–C1 143.1(3), N1–C7 133.3(3), N1···Cl1 309.7(1), N1–H···Cl1 221.4(4), N2–C7 134.4(3), N2–C8 147.6(3), N3–C8 142.9(3), N3–C9 136.6(4), N4–C9 136.8(4), N4–C10 144.3(4), N5–C7 133.9(3), N5–C10 145.7(3), N6–C2 143.1(3), N6–C15 133.3(4), N6···Cl2 309.4(3), N6–H···Cl2 221.7(4), N7–C15 134.1(3), N7–C16 146.6(4), N8–C16 143.4(4), N8–C17 137.1(4), N9–C17 137.7(4), N9–C18 144.3(3), N10–C15 134.1(3), N10–C18 146.7(4), C9–O1 122.3(3), C17–O2 122.2(3), C1–C2 140.2(4), C8–C10 153.9(4), C16–C18 146.7(4), C1–N1–C7 127.2(2), N2–C7–N5 112.0(2), N3–C9–N4 108.4(2), C2–N6–C15 126.2(2), N10–C15–N7 111.9(2), N8–C17–N9 108.0(2). b) 1D networks of $(\mathbf{1}H_2)Cl_2{\cdot}H_2O$.

Monoprotonation of **1** to give $[\mathbf{1}H]PF_6$ was achieved by reaction of **1** with NH_4PF_6. However, no crystals of this salt could be obtained. Therefore, a salt exchange reaction

with $NaBPh_4$ was carried out. The resulting [**1**H]BPh_4 was crystallized from CH_3OH solution (Figure 5, a). As anticipated, the proton binds to the imino N atom, which is the most basic site. The data argue against a bridging position of the proton between the two imino N atoms, implying that **1** does not meet the criteria set for a proton sponge. The N=C bond length within the protonated guanidino unit was determined to be 133.1(2) pm, which is significantly longer than the N=C distance within the second, unprotonated guanidino group [128.8(2) pm]. Protonation resulted in a decrease of the N···N separation between the imino N atoms of the two guanidino groups from 295.3(5) pm before protonation to 287.9(4) pm after. A similar decrease [from 285.8(2) to 276.8(3) pm] was observed upon protonation of btmgb.[13] The tetraprotonated (reaction with HCl) and diprotonated (reaction with NH_4PF_6) molecules of **2** were also synthesized. Again the spectroscopic data indicate protonation of the imino N atoms. The molecular structure of [**2**H_2]BPh_4 is shown in Figure 5 (b). As anticipated, two guanidino groups in *para*-positions to each other are protonated. An important detail, which diprotonated **2** shares with monoprotonated **1**, is that the orientation of the N–H bond is away from the imino N atom of the adjacent guanidino group. Hence **2** does not qualify as a proton sponge either.

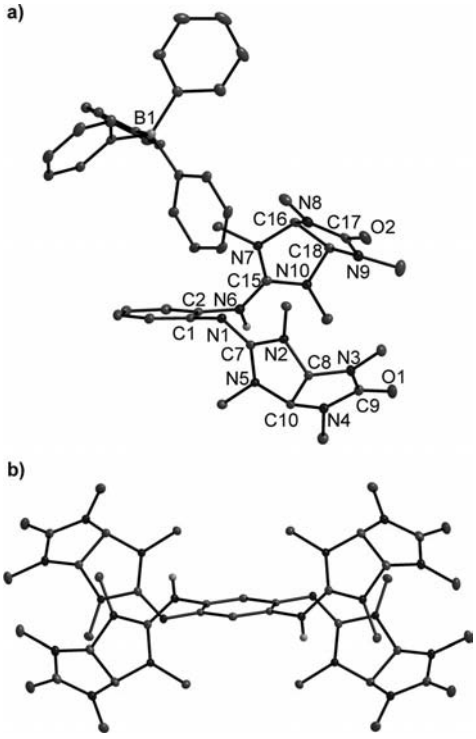

Figure 5. Molecular structures of (**1**H)BPh_4 and (**2**H_2)$(BPh_4)_2$ (only the dication is shown) (hydrogen atoms attached to carbon atoms omitted for clarity). Vibrational ellipsoids are drawn at 50% probability. a) Selected structural parameters (bond lengths in pm, bond angles in °) for (**1**H)BPh_4: N1–C1 139.6(2), N1–C7 128.8(2), N2–C7 137.0(2), N2–C8 144.4(2), N3–C8 144.6(2), N3–C9 135.3(2), N4–C9 136.6(2), N4–C10 144.8(2), N5–C7 137.8(2), N5–C10 145.3(2), N6–C2 143.8(2), N6–C15 133.1(2), N7–C15 133.7(2), N7–C16 146.3(2), N8–C16 144.1(2), N8–C17 136.8(3), N9–C17 137.5(2), N9–C18 144.1(2), N10-C15 133.8(2), N10-C18 146.8(2), O1–C9 123.5(2), O2–C17 121.6(2), C1–C2 140.5(3), C8–C10 154.4(2), C16-C18 154.7(3), C1–N1–C7 125.00(15), N2–C7–N5 107.96(15), N3–C9–N4 109.19(14), C2–N6–C15 124.78(15), N7–C15–N10 111.50(15), N8–C17–N9 107.89(16). b) Selected structural parameters (bond lengths in pm, bond angles in °): N1–C1 142.8(2), N1–C4 132.5(2), N2–C4 133.7(2), N2–C5 145.9(3), N3–C5 144.2(3), N3–C6 135.8(3), N4–C6 136.1(3), N4–C7 144.7(3), N5–C4 134.6(2), N5–C7 145.8(2), N6–C3 141.4(2), N6–C12 130.4(2), N7–C12 136.2(2), N7–C13 145.0(2), N8–C13 144.2(3), N8–C14 136.2(3), N9–C14 136.0(3), N9–C15 144.0(3), N10–C12 136.5(2), N10–C15 144.8(2), C6–O1 123.7(2), C14–O2 123.2(2), C5–C7 154.0(3), C13–C15 154.7(3), C1–C2 138.5(3), C1–C3′ 140.5(3), C2–C3 139.3(3), C1–N1–C4 124.45(17), C3–N6–C12 122.35(16), N2–C4–N5 111.48(17), N3–C6–N4 109.26(17), N7–C12–N10 109.04(16), N8–C14–N9 108.58(17).

Redox Properties

The introduction of guanidino groups in *para*-positions to each other as in **2** leads to an easily oxidized system. The cyclic voltammogram (CV) of **2**, measured in CH_3CN vs. the saturated calomel electrode (SCE) at a scan speed of 50 mV s^{-1}, is displayed in Figure 6 (upper trace), and shows a sharp two-electron wave (**2**/**2**$^{2+}$) at $E_{1/2}(CH_3CN)$ = –0.15 V vs. SCE (E_{ox} = –0.11 V and E_{red} = –0.18 V). In comparison, –0.32 V was measured for that of ttmgb,[18] and –0.36 V for tdmegb.[24] Thus in CH_3CN solutions **2** is a slightly weaker electron donor than ttmgb or tdmegb. In addition, a second wave was observed (at ca. $E_{1/2}$ = +1.15 V), which appears to arise from an irreversible redox process. The lower trace in Figure 6 was measured in CH_2Cl_2 solution, yielding $E_{1/2}(CH_2Cl_2)$ = –0.11 V vs. SCE (E_{ox} = –0.02 V and E_{red} = –0.19 V). Ferrocene was added as internal standard, giving $E_{1/2}(CH_2Cl_2)$ = –0.62 vs. Fc/Fc^+.

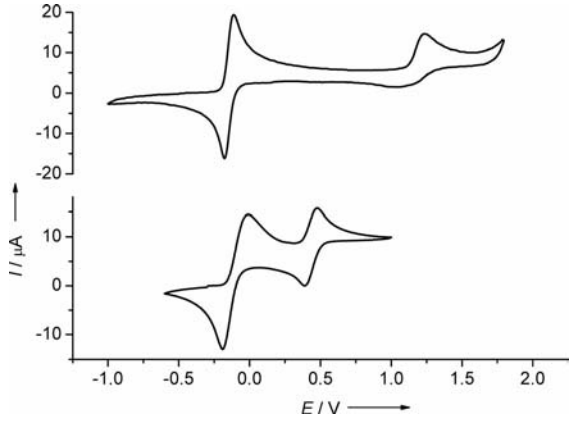

Figure 6. CV for **2** measured at a scan rate of 50 mV s^{-1} vs. SCE. Upper trace: CH_3CN solution. Lower trace: CH_2Cl_2 solution in the presence of ferrocene.

Aerial oxidation proceeded slowly and resulted in a characteristic green color of CH_2Cl_2 solutions of **2** exposed to air for a prolonged time. Oxidation of **2** by I_2 was analysed. Upon addition of two equivalents of I_2 to **2** dissolved in CH_3CN, the solution adopted the characteristic green color, which is also observed upon oxidation of ttmgb or tdmegb.

Dark crystals of $(\mathbf{2})(I_3)_2 \cdot 2CH_3CN$ suitable for X-ray diffraction, formed according to Equation (2), were grown from this solution, and Figure 7 (a) shows the structure.

$$\mathbf{2} + 3\,I_2 \longrightarrow (\mathbf{2})(I_3)_2 \qquad (2)$$

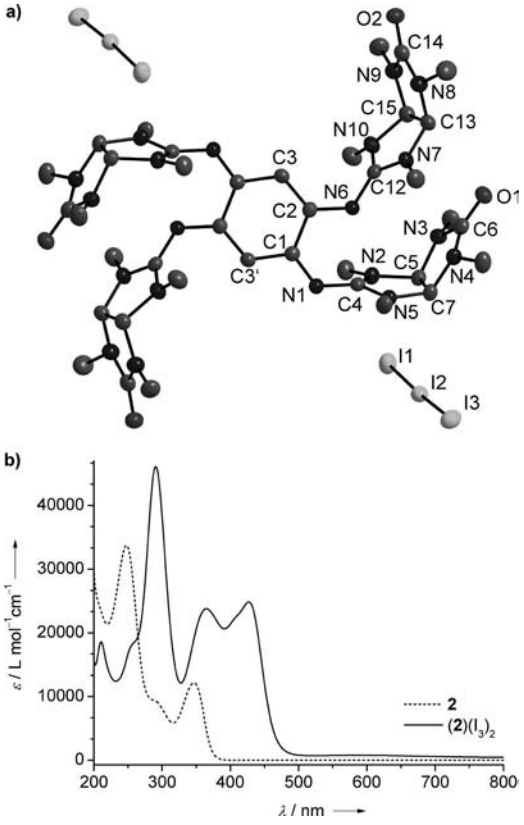

Figure 7. a) Molecular structure of $\mathbf{2}(I_3)_2 \cdot 2CH_3CN$ (hydrogen atoms omitted for clarity). Vibrational ellipsoids are drawn at 20% probability. Selected structural parameters (bond lengths in pm, bond angles in °): N1–C1 130.6(5), N1–C4 134.8(5), N2–C4 132.8(5), N2–C5 147.7(5), N3–C5 144.1(5), N3–C6 137.9(5), N4–C6 136.3(5), N4–C7 144.0(5), N5–C4 133.4(5), N5–C7 147.2(5), N6–C2 134.4(5), N6–C12 133.9(5), N7–C12 134.2(5), N7–C13 144.2(5), N8–C13 145.2(5), N8–C14 139.1(5), N9–C14 136.1(5), N9–C15 142.0(5), N10–C12 135.2(5), N10–C15 146.9(5), C6–O1 122.0(4), C14–O2 123.0(5), C5–C7 154.5(5), C13-C15 153.8(6), C1–C2 149.6(5), C1–C3′ 141.8(5), C2–C3 138.7(5), I1–I2 298.66(6), I2–I3 287.68(6), C1–N1–C4 125.8(3), C2–N6–C12 123.3(3), N2–C4–N5 111.8(3), N3–C6–N4 108.6(3), N7–C12–N10 110.4(3), N8–C14–N9 108.6(3), I1–I2–I3 177.184(12). b) UV/Vis spectra of **2** and $(\mathbf{2})(I_3)_2$ in CH_3CN.

The arrangement of the four guanidino units around the C_6 ring resembles a paddle wheel. The C–C bond lengths within the central C_6 ring of 149.6(5) (C1–C2), 141.8(5) (C1–C3′), and 138.7(5) pm (C2–C3) clearly indicate the loss of aromaticity. As with the related species ttmgb and tdmegb, oxidation resulted in removal of two electrons from the aromatic π system. The dication is best described as a pair of bisguanidinoallyl cations connected by two C–C single bonds. The C=N double bonds were elongated to 134.8(5) and 133.9(5) pm upon oxidation. In the UV/Vis spectrum of $(\mathbf{2})(I_3)_2$ (Figure 7, b) absorptions belonging to the dicationic ligand are visible at 211, 255, and 427 nm. Another extremely broad, weak feature appeared at around 600 nm. In addition, two typically strong bands due to I_3^- were observed at 290 and 364 nm.[37]

Coordination Chemistry

As already discussed, **1** and **2** are extremely amenable to protonation. In the case of **2**, redox reactions generally compete with coordination. In the light of problems arising from product mixtures, crystallization was found to be the best method for purification of the coordination products. Therefore, we restrict the discussion mainly to experiments in which crystalline products were obtained in relatively high yield (generally suitable for a single-crystal X-ray diffraction analysis). We started with the reaction of **1** with $[PtCl_2(dmso)_2]$ in CH_2Cl_2, which yielded the orange complex $[(\mathbf{1})PtCl(dmso)][PtCl_3(dmso)]$; see Equation (3).

$$\mathbf{1} + 2\,[PtCl_2(dmso)_2] \xrightarrow[-\,2\ dmso]{} [(\mathbf{1})PtCl(dmso)][PtCl_3(dmso)] \qquad (3)$$

$$\mathbf{2} + 4\,[PtCl_2(dmso)_2] \xrightarrow[-\,4\ dmso]{} [(\mathbf{2})\{PtCl(dmso)\}_2][PtCl_3(dmso)]_2 \qquad (4)$$

This compound was crystallized by the diffusion of Et_2O into a CH_2Cl_2 solution. The structure of one of the ion pairs is reproduced in Figure 8 (a). Both guanidino groups were bound to the Pt^{II} center through the imino N atoms, realizing a $\kappa^2(N,N')$ coordination mode. As anticipated, the Pt atom was four-coordinate in a planar fashion, with Pt–N bond lengths of 200.4(2) and 201.9(2) pm. The N=C bond lengths (ca. 138 pm) were significantly elongated with respect to free **1** [129.13(14) pm], indicative of the presence of π-bonding.[16] The UV/Vis spectrum (Figure 9) featured a broad band at around 460 nm, responsible for the orange color of the complex. As a result of coordination, the bands of the free ligand at 225, 267, and 306 nm are redshifted to 229, 286, and 331 nm. For comparison, in the UV/Vis spectrum recorded for $[(btmgb)PtCl(dmso)][PtCl_3(dmso)]$, a broad band appeared at 431 nm, and two sharper features are seen at 292 and 341 nm.[13] A similar reaction, with **2** furnished dinuclear $[(\mathbf{2})\{PtCl(dmso)\}_2][PtCl_3(dmso)]_2$ [Equation (4)], and its UV/Vis spectrum is also shown in Figure 9. Unfortunately, crystals suitable for an XRD study were not obtained.

Reaction of **2** with $[PtCl_2(C_2H_4)]_2$ afforded $[(\mathbf{2})\{PtCl(C_2H_4)\}_2][PtCl_3(C_2H_4)]_2$; see Equation (5). Crystals of sufficient quality for XRD analysis were obtained.

$$\mathbf{2} + 2\,[PtCl_2(C_2H_4)]_2 \longrightarrow [(\mathbf{2})\{PtCl(C_2H_4)\}_2][PtCl_3(C_2H_4)]_2 \qquad (5)$$

The dicationic unit is shown in part b of Figure 8. The two ethylene ligands adopt a *trans*-conformation and the molecule possesses a center of inversion. The XRD derived structure heavily underestimates the ethylene C=C bond lengths [122.4(2) pm], which is a well known problem with ethylene complexes.[19] At 202.0(5) and 202.1(5) pm, the two Pt–N bond lengths are virtually identical and similar to those in the mononuclear complex $[(\mathbf{1})PtCl(dmso)]^+$. The considerable elongation of the C=N imino bonds [from 128.7(2)/128.8(2) pm before to 135.3(8) pm after complex-

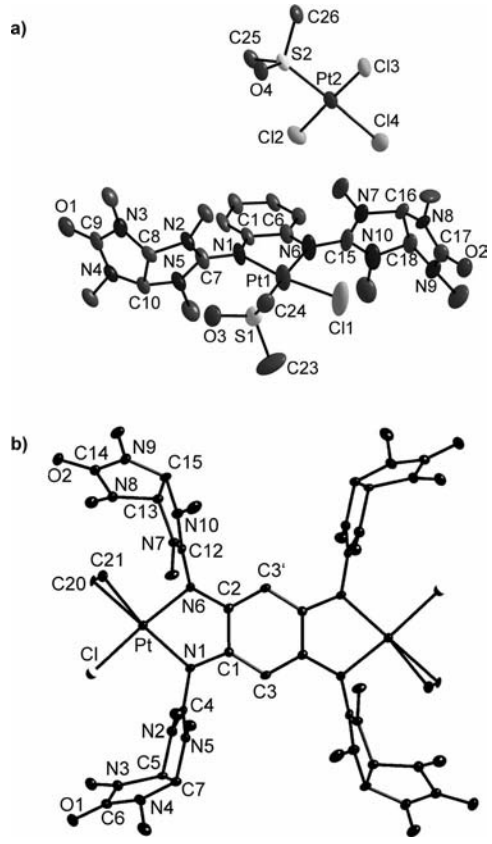

Figure 8. Molecular structures of [(**1**)PtCl(dmso)][$PtCl_3$(dmso)] and [(**2**){PtCl(C_2H_4)}$_2$][$PtCl_3(C_2H_4)]_2$ (hydrogen atoms omitted for clarity). Vibrational ellipsoids are drawn at 20% probability. a) Selected structural parameters (bond lengths in pm, bond angles in °) for [(**1**)PtCl(dmso)][$PtCl_3$(dmso)]: Pt1–N1 200.4(16), Pt1–N6 201.9(15), Pt1–Cl1 232.6(8), Pt1–S1 220.3(5), N1–C1 140(2), N1–C7 138.0(18), N2–C7 130(2), N2–C8 146.4(18), N3–C8 142(2), N3–C9 134(2), N4–C9 136(2), N4–C10 140(2), N5–C7 132(2), N5–C10 147.6(17), N6–C6 135(2), N6–C15 138(2), N7–C15 132(3), N7–C16 146(2), N8–C16 144(3), N8–C17 130(3), N9–C17 134(3), N9–C18 145(2), N10-C15 131(3), N10-C18 144(3), C1–C6 141(2), C8–C10 157(2), C16-C18 157(3), C9–O1 124(2), C17–O2 127(2), S1–O3 146.5(15), S1–C23 181(3), S1–C24 179(2), Pt2–Cl2 229.6(5), Pt2–Cl3 231.6(4), Pt2–Cl4 231.5(6), Pt2–S2 218.5(4), S2–O4 147.2(9), S2–C25 176.9(16), S2–C26 177.3(18), N1–Pt1–N6 78.1(6), Cl1–Pt1–S1 89.5(2), C1–N1–C7 119.6(15), C6–N6–C15 122.6(15), N2–C7–N5 113.3(13), N3–C9–N4 109.2(17), N7–C15–N10 112(2), N8–C17–N9 114(2). b) Selected structural parameters (bond lengths in pm, bond angles in °) for [(**2**){PtCl(C_2H_4)}$_2$][$PtCl_3(C_2H_4)]_2$: Pt–Cl 230.0(2), Pt–C20 217.1(5), Pt–C21 213.8(8), Pt–N1 202.0(5), Pt–N6 202.1(5), N1–C1 143.1(8), N1–C4 135.3(8), N2–C4 134.3(8), N2–C5 145.2(8), N3–C5 144.6(9), N3–C6 136.0(8), N4–C6 138.0(9), N4–C7 143.3(9), N5–C4 134.0(8), N5–C7 147.2(8), N6–C2 141.9(8), N6–C12 135.3(8), N7–C12 134.8(8), N7–C13 146.5(8), N8–C13 144.5(9), N8–C14 138.8(9), N9–C14 134.9(10), N9–C15 142.5(8), N10–C12 132.3(8), N10–C15 148.0(8), C1–C2 140.3(9), C1–C3 138.1(9), C2–C3′ 139.9(9), O1–C6 122.4(8), O2–C14 122.1(8), C20–C21 122.4(2), N1–Pt–N6 80.1(2), C20–Pt–C21 33.0(3), Cl–Pt–N1 95.91(16), C1–N1–C4 120.3(5), C2–N6–C12 119.7(5).

ation] again signals significant π-bond contributions. Thermogravimetric analysis (TGA, Supporting Information) indicated that the complex is stable up to ca. 180 °C. Loss of the ethylene ligands took place at ca. 200 °C. Finally, after heating to 450 °C, only elemental Pt remained.

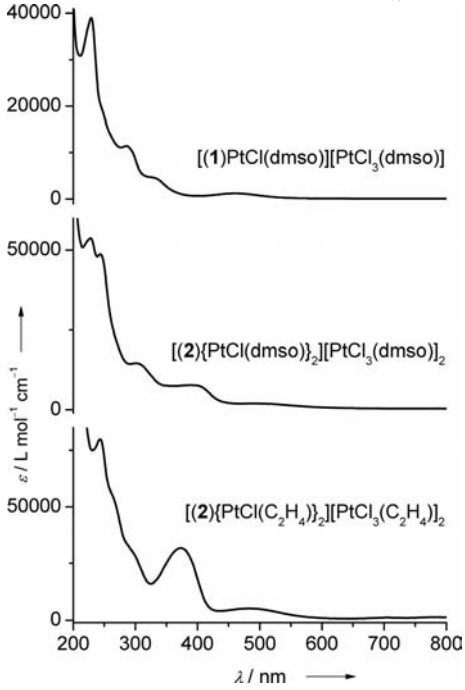

Figure 9. UV/Vis spectra of [(**1**)PtCl(dmso)][$PtCl_3$(dmso)], [(**2**){PtCl(dmso)}$_2$][$PtCl_3$(dmso)]$_2$, and [(**2**){PtCl(C_2H_4)}$_2$][$PtCl_3$-(C_2H_4)]$_2$ in CH_3CN.

Subsequently, we prepared the two mononuclear complexes [(**1**)$NiCl_2$] and [(**1**)$PdCl_2$]. [(**1**)$NiCl_2$] was the product of the reaction between [(dme)$NiCl_2$] (dme = 1,2-dimethoxyethylene) and **1**; see Equation (6). [(**1**)$PdCl_2$] was obtained from [(cod)$PdCl_2$] (cod = 1,5-cyclooctadiene) and **1**; see Equation (7).

1 + [(dme)$NiCl_2$] $\xrightarrow[-\text{ dme}]{}$ [(**1**)$NiCl_2$] (6)

1 + [(cod)$PdCl_2$] $\xrightarrow[-\text{ cod}]{}$ [(**1**)$PdCl_2$] (7)

2 + 2 [(dme)$NiCl_2$] $\xrightarrow[-\text{ 2 dme}]{}$ [(**2**)$(NiCl_2)_2$] (8)

2 + 2 [(cod)$PdCl_2$] $\longrightarrow$ product mixture (9)

The UV/Vis spectrum of green [(**1**)$PdCl_2$] in CH_3CN contains weak bands at λ = 425 and 605 nm with extinction coefficients of 594 and 838 $L\,mol^{-1}\,cm^{-1}$ (in addition to strong bands centred at λ = 231, 299, and 333 nm), which can be assigned to transitions involving the Pd d-orbitals (see Supporting Information). Both complexes were crystallized and structurally characterized (Figure 10). The orientation of the guanidino groups is relatively flexible (formal rotation around the C=N double bond) so the ligand can react to the different steric situations in the tetrahedral Ni^{II} complex and the planar Pd^{II} complex. The Ni–N bond lengths of 199.9(2) and 200.0(2) pm in [(**1**)$NiCl_2$] fell in the characteristic region and are similar to those reported for [(btmgb)$NiCl_2$][16] and [(bdmegb)$NiCl_2$].[15] With 83.7(1)°, the N–Ni–N angle is relatively small. The Cl–Ni–Cl angle is quite large [127.69(4)°]. Such large angles (significantly larger than the ideal tetrahedral angle of 109.4°) were found

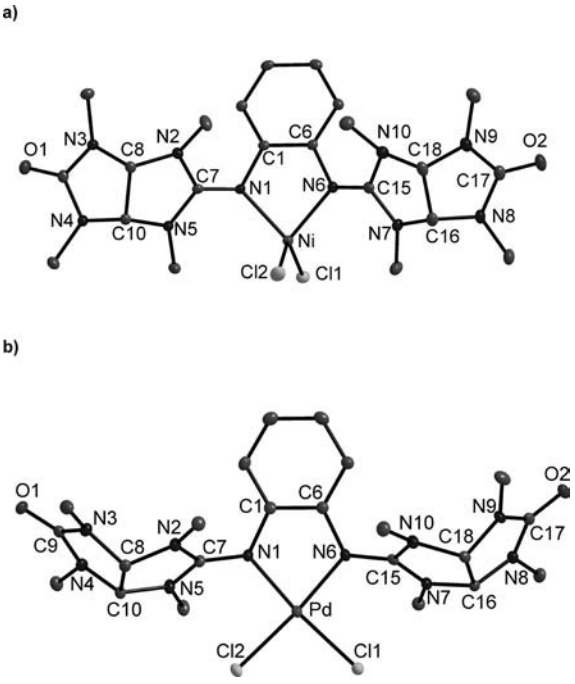

Figure 10. Molecular structures of [(**1**)$NiCl_2$] and [(**1**)$PdCl_2$] (hydrogen atoms omitted for clarity). Vibrational ellipsoids are drawn at 20% probability. a) Selected structural parameters (bond lengths in pm, bond angles in °) for [(**1**)$NiCl_2$]: Ni–Cl1 225.77(10), Ni–Cl2 221.12(11), Ni–N1 199.9(2), Ni–N6 200.0(2), N1–C1 142.9(4), N1–C7 131.8(4), N2–C7 136.9(4), N2–C8 145.7(4), N3–C8 144.8(4), N3–C9 135.1(4), N4–C9 138.0(4), N4–C10 143.9(4), N5–C7 134.4(4), N5–C10 145.8(4), N6–C6 141.6(4), N6–C15 131.2(4), N7–C15 134.1(4), N7–C16 144.7(4), N8–C16 144.7(4), N8–C17 136.9(5), N9–C17 134.4(5), N9–C18 143.9(4), N10–C15 138.0(4), N10–C18 146.4(4), O1–C9 122.7(4), O2–C17 122.9(4), C1–C6 140.1(4), Cl1–Ni–Cl2 127.69(4), N1–Ni–N6 83.72(10), C1–N1–C7 120.1(2), C6–N6–C15 122.5(3). b) Selected structural parameters (bond lengths in pm, bond angles in °) for [(**1**)$PdCl_2$]: Pd–Cl1 230.71(13), Pd–Cl2 230.16(11), Pd–N1 203.8(4), Pd–N6 203.0(3), N1–C1 141.0(5), N1–C7 134.2(5), N2–C7 133.5(5), N2–C8 146.4(5), N3–C8 143.3(6), N3–C9 136.6(6), N4–C9 138.0(6), N4–C10 144.2(6), N5–C7 133.9(5), N5–C10 145.3(5), N6–C6 141.5(6), N6–C15 134.4(5), N7–C15 133.1(5), N7–C16 145.7(5), N8–C16 143.4(5), N8–C17 136.1(6), N9–C17 137.5(6), N9–C18 143.1(5), N10–C15 134.5(5), N10–C18 146.3(5), O1–C9 122.2(5), O2–C17 122.3(5), C1–C6 141.0(6), Cl1–Pd–Cl2 90.54(4), N1–Pd–N6 80.32(14), C1–N1–C7 120.5(4), C6–N6–C15 119.7(3).

in the majority of tetrahedrally coordinated Ni^{II} dichloride complexes with chelating N-donor ligands, arguing for electronic reasons rather than crystal packing effects (see preliminary discussion in Ref.[15]).[38] The dinuclear complex [**2**$(NiCl_2)_2$] was prepared by reaction of **2** with [(dme)$NiCl_2$] in CH_3CN; Equation (8). Pink needle-shaped crystals were obtained by diffusion of Et_2O into a CH_2Cl_2 solution of the complex, which were not suitable for XRD analysis. The UV/Vis spectra of [(**1**)$NiCl_2$] (green) and [**2**$(NiCl_2)_2$] (pink) are shown in Figure 11. Strong absorptions appear below 350 nm, with maxima at 250, 288, and 306 (shoulder) nm for [(**1**)$NiCl_2$] and 252, 274, 317, and 341 nm for [**2**$(NiCl_2)_2$]. These absorptions belong to transitions mainly localized at the aromatic and guanidino groups. In addition, weak bands occur at lower energy [439, 513, 577, and 699 nm for {(**1**)$NiCl_2$} and 466, 529, 591, and 702 nm for {**2**$(NiCl_2)_2$}], which can be assigned tentatively to d–d transitions at Ni^{II}. In line with this assignment, the extinction coefficients of these bands are about twice as large for [**2**$(NiCl_2)_2$] than for [(**1**)$NiCl_2$]. In comparison, the UV/Vis spectrum of [(ttmgb)$(NiCl_2)_2$] features weak bands centred at 480, 575, 685, and 1025 nm.[15] The reaction of **2** with [(cod)$PdCl_2$] resulted in a mixture from which it was impossible to obtain a clean product; see Equation (9). The color of the solution indicated that coordination competed with redox processes in this case.

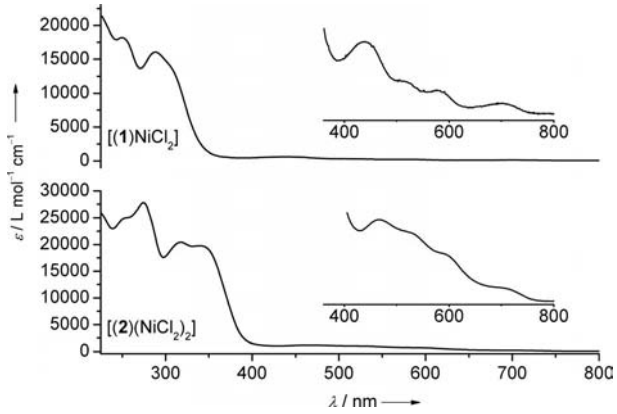

Figure 11. UV/Vis spectra of a) [(**1**)$NiCl_2$] and b) [**2**$(NiCl_2)_2$] in CH_2Cl_2.

The reaction between **2** and [$PdCl(\eta^3\text{-}C_3H_5)]_2$ in $CHCl_3$ furnished [**2**$\{Pd(\eta^3\text{-}C_3H_5)\}_2$][$PdCl_2(\eta^3\text{-}C_3H_5)]_2$ in more than 60% yield as yellow needle-shaped crystals. To allow a direct comparison, the corresponding mononuclear complex [(**1**)$Pd(\eta^3\text{-}C_3H_5)$][$PdCl_2(\eta^3\text{-}C_3H_5)$] was also synthesized; see Equations (10) and (11).

$$\mathbf{1} + [PdCl(\eta^3\text{-}C_3H_5)]_2 \longrightarrow [(\mathbf{1})Pd(\eta^3\text{-}C_3H_5)][PdCl_2(\eta^3\text{-}C_3H_5)] \quad (10)$$

$$\mathbf{2} + 2\,[PdCl(\eta^3\text{-}C_3H_5)]_2 \longrightarrow [(\mathbf{2})\{Pd(\eta^3\text{-}C_3H_5)\}_2][PtCl_2(\eta^3\text{-}C_3H_5)]_2 \quad (11)$$

The UV/Vis spectrum of [(**1**)$Pd(\eta^3\text{-}C_3H_5)$][$PdCl_2(\eta^3\text{-}C_3H_5)$] in CH_2Cl_2 features three bands centred near 234, 291, and 383 nm (see Supporting Information). In the case of [**2**$\{Pd(\eta^3\text{-}C_3H_5)\}_2$][$PdCl_2(\eta^3\text{-}C_3H_5)]_2$, bands centred at 241, 289, 363, and 435 (weak and broad) nm were measured (see Supporting Information). The molecular structures of both allyl complex cations are shown in Figure 12. In line with several other cationic η^3-coordinated allyl–Pd complexes,[39] the bond lengths between Pd and all three C atoms of the allyl ligand are similar. The C–C–C bond angle in the allyl group is close to 120°. The angle between the allyl plane and the N–Pd–N plane amounts to 115° for $[(\mathbf{1})Pd(\eta^3\text{-}C_3H_5)]^+$ and 109° for $[(\mathbf{2})\{Pd(\eta^3\text{-}C_3H_5)\}_2]^{2+}$. In comparison, in $[PdCl_2(\eta^3\text{-}C_3H_5)]^-$ the angle between the $PdCl_2$ plane and the allyl plane is 117° for the mono- and 118° for the dinuclear complex. The thermal stability of the two allyl complexes in the solid state was assessed by TGA. The resulting curves are plotted in Figure 13. The step at 100 °C in the curve of [**2**$\{Pd(\eta^3\text{-}C_3H_5)\}_2$][$PdCl_2(\eta^3\text{-}C_3H_5)]_2\cdot 2CH_2Cl_2$ (bottom) arises from the loss of the

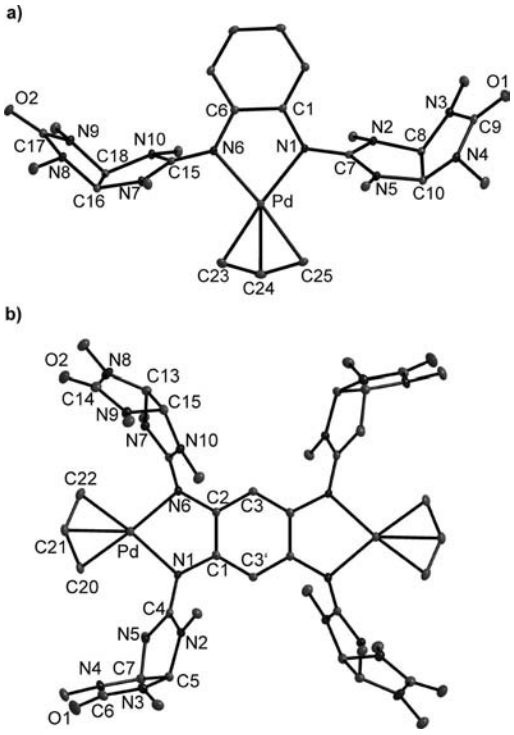

Figure 12. Molecular structures of $[(\mathbf{1})Pd(\eta^3\text{-}C_3H_5)][PdCl_2(C_3H_5)]$ (only the cation is shown) and $[(\mathbf{2})\{Pd(\eta^3\text{-}C_3H_5)\}_2][PdCl_2(C_3H_5)]_2$ (only the dication is shown). Hydrogen atoms omitted for clarity. Vibrational ellipsoids are drawn at 20% probability. a) Selected structural parameters (bond lengths in pm, bond angles in °) for $[(\mathbf{1})Pd(\eta^3\text{-}C_3H_5)][PdCl_2(C_3H_5)]$: Pd–N1 208.1(2), Pd–N6 210.3(2), Pd–C23 211.5(3), Pd–C24 210.5(3), Pd–C25 211.9(3), N1–C1 141.9(3), N1–C7 133.1(3), N2–C7 135.8(3), N2–C8 145.3(3), N3–C8 144.2(4), N3–C9 137.3(3), N4–C9 138.6(4), N4–C10 144.1(3), N5–C7 134.3(3), N5–C10 147.0(3), N6–C6 141.6(3), N6–C15 132.5(3), N7–C15 136.0(3), N7–C16 145.8(3), N8–C16 144.3(4), N8–C17 138.9(4), N9–C17 137.3(4), N9–C18 143.5(3), N10–C15 135.2(3), N10–C18 146.8(3), O1–C9 121.5(3), O2–C17 121.5(3), C1–C6 140.8(4), N1–Pd–N6 79.39(9), C23–Pd–C25 69.11(12), C1–N1–C7 120.6(2), N2–C7–N5 110.5(2), C6–N6–C15 121.1(2), N7–C15–N10 110.4(2), C23–C24–C25 117.8(3). b) Selected structural parameters (bond lengths in pm, bond angles in °) for $[(\mathbf{2})\{Pd(\eta^3\text{-}C_3H_5)\}_2][PdCl_2(C_3H_5)]_2$: Pd–N1 210.7(3), Pd–N6 211.8(3), Pd–C20 210.6(4), Pd–C21 212.8(4), Pd–C22 212.9(4), O1–C6 121.5(5), O2–C14 122.1(5), N1–C1 143.8(4), N1–C4 131.4(5), N2–C4 135.1(5), N2–C5 147.4(5), N3–C5 143.9(5), N3–C6 137.3(5), N4–C6 137.8(5), N4–C7 145.2(5), N5–C4 136.6(5), N5–C7 145.0(5), N6–C2 142.7(4), N6–C12 132.1(5), N7–C12 136.8(5), N7–C13 146.0(5), N8–C13 143.4(5), N8–C14 138.1(6), N9–C14 137.2(5), N9–C15 146.0(5), N10–C12 135.9(5), N10–C15 144.2(5), C1–C2 140.3(5), C1–C3′ 138.6(5), C2–C3 138.8(5), N1–Pd–N6 80.04(11), C20–Pd–C22 68.39(16), C1–N1–C4 120.8(3), N2–C4–N5 109.9(3), C2–N6–C12 119.6(3), N7–C12–N10 109.9(3), C20–C21–C22 116.7(4).

cocrystallized CH_2Cl_2. The allyl complexes were stable up to ca. 200 °C. Decomposition occurred in three steps; in the first step (at ca. 200 °C) the allyl groups were eliminated. It follows that a possible decomposition pathway involving reductive elimination with allylation of the guanidine imino N atom and formation of Pd^0 could be excluded. A similar decomposition has been studied for N-heterocyclic carbene-stabilized Pd^{II} allyl complexes, which lead to 2-allylimidazolium salts.[39a,40] For the complexes synthesized here there is no evidence (TGA or NMR) for the allylation of the guanidine ligand. The total mass loss after reaching a temperature of 400 °C in the TGA curve of $[(\mathbf{2})\{Pd(\eta^3\text{-}C_3H_5)\}_2][PdCl_2(\eta^3\text{-}C_3H_5)]_2\cdot 2CH_2Cl_2$ indicates complete decomposition, with black elemental Pd being the only remaining solid. In the case of $[(\mathbf{1})Pd(\eta^3\text{-}C_3H_5)][PdCl_2(\eta^3\text{-}C_3H_5)]$, a brown solid remained, presumably $Pd/PdCl_2$.

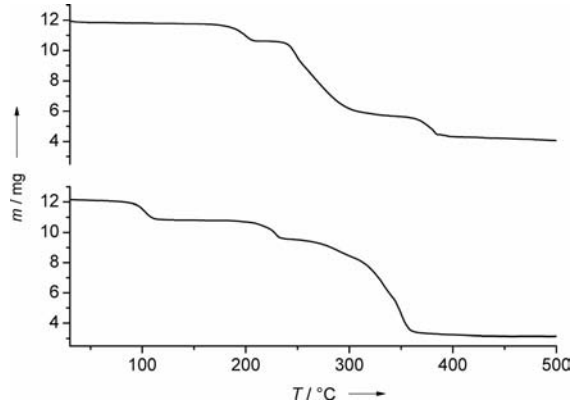

Figure 13. TGA curves for $[(\mathbf{1})Pd(\eta^3\text{-}C_3H_5)][PdCl_2(C_3H_5)]$ (top) and $[(\mathbf{2})\{Pd(\eta^3\text{-}C_3H_5)\}_2][PdCl_2(C_3H_5)]_2\cdot 2CH_2Cl_2$ (bottom).

As already mentioned, the introduction of bulky guanidino groups in **1** and **2** could be of interest for catalytic applications. The catalytic activity of complexes of these two and related ligands will be studied in more detail in future work. In initial test experiments, we applied the mononuclear complex $[(\mathbf{1})NiCl_2]$ to ethylene oligomerization. Ethylene was passed over a mixture of $[(\mathbf{1})NiCl_2]$ and ca. 3000 equiv. of methylaluminoxane in toluene. After 38 min, the reaction was quenched by addition of EtOH/HCl. The organic phase was washed three times with H_2O/HCl, and analysed by GC/MS. Oligomerization to C_6–C_{11} hydrocarbons (mostly C_6 with 77%) with an activity of approx. 1600 $g\,mmol^{-1}$ (Ni) h^{-1} was found.

Conclusions

We reported the synthesis of two new diimine ligands **1** and **2** featuring bulky bicyclic guanidino groups. Of these, **2** was shown to be a relatively strong electron donor. Oxidation of **2** with I_2 led to the triiodide salt of the dication, which could be described as a pair of bisguanidinoallyl cations connected by two C–C single bonds. Protonation experiments were carried out with the strongly basic guanidines, showing that protonation occurs exclusively at the imino N atoms indicating that the new ligands are not proton sponges. Several mononuclear (in the case of **1**) and dinuclear (in the case of **2**) Ni, Pd, and Pt metal complexes, all featuring a chelating coordination mode, were synthesized and characterized. In these complexes, the bulky bicyclic guanidino groups shield the metal center from two sides. Initial test experiments were carried out in which a Ni complex was applied to catalytic ethylene oligomerization. The activity was moderate, and C_6 hydrocarbons were mostly formed. In our ongoing work we are replacing the

methyl groups at the bicyclic guanidino groups with more space-demanding alkyl or aryl groups to test the influence of such substitutions on the catalytic activity. Future work will also focus on the redox chemistry of **2** and its donor–acceptor properties.

Experimental Section

General: All the synthetic work was carried out under an Ar atmosphere using standard Schlenk techniques. All solvents were dried by standard methods prior to their use. NMR spectra were measured with a Bruker DPX 200, Avance II 400, or Avance III 600 spectrometer. A Cary 5000 spectrophotometer was used for UV/Vis spectroscopy. CsI discs of the compounds were measured with a FT-IR Biorad Merlin Excalibur FT 3000 spectrometer. Elemental analyses were carried out at the Microanalytical Laboratory of the University of Heidelberg. A EG&G Princeton 273 apparatus was used for the CV measurements. The curves were recorded at different scan rates in the range 50–200 mV s^{-1} using a SCE as the reference electrode and Bu_4NPF_6 (Fluka, electrochemical grade) as the electrolyte. TGA were carried out with a Mettler TC15 under Ar in the range 30–500 °C. A Finnigan MAT 8230 (FAB) or a Bruker ApexQe FT-ICR (ESI) were used for mass spectrometry (MS).

Bicyclic Tetramethylbisurea: To CH_3OH (200 mL) and glyoxal solution (2.3 mL, 20 mmol, 40% in H_2O) were added concentrated HCl (1 mL) and $(MeHN)_2CO$ (3.6 g, 40.9 mmol) in methanol (200 mL). After heating the reaction mixture to reflux for 30–45 min, it was stirred for additional 20 h at room temp. After removal of the solvent a colorless solid was obtained, which was recrystallized from CH_3OH and washed with Et_2O. The colorless crystals were dried at 60 °C under high vacuum; yield 2.228 g (11.2 mmol, 56%). ^1H NMR (399.89 MHz, $CDCl_3$, 295.5 K): δ = 4.91 (s, 2 H, CH), 2.95 (s, 12 H, CH_3) ppm. ^{13}C NMR (100.56 MHz, $CDCl_3$, 297.1 K): δ = 158.69 (CO), 72.05 (CH), 30.39 (CH_3) ppm. The product was used for the preparation of **1** and **2** without further analysis.

Ligand 1: Bicyclic tetramethylbisurea (1.356 g, 6.84 mmol) was suspended in toluene (40 mL). After addition of oxalylchloride (6.6 mL, 75.7 mmol) via syringe, the reaction mixture was heated to 80–90 °C for 20 h. The solvent was removed under vacuum, and the residue washed 3–4 times with Et_2O. A beige product (1.264 g) was obtained, which consisted of ca. 40% activated and 60% deactivated bisurea; yield 2.04 mmol, 29.8%. ^1H NMR (200 MHz, $CDCl_3$, 295.0 K): δ = 6.28 (s, 2 H, CH), 3.49 (s, 6 H, CH_3), 3.07 (s, 6 H, CH_3) ppm. The activated bisurea was dissolved in CH_3CN (8 mL), and triethylamine (0.55 mL, 4 mmol) and a solution of 1,2-diaminobenzene (108 mg, 1 mmol) in CH_3CN (6 mL) were added by syringe. After 30 min, an NaOH solution (0.86 mL, 25% in H_2O) was added dropwise to the reaction mixture, and the solvent was removed under high vacuum. The remaining residue was suspended in H_2O and filtered. The collected solid was dissolved (if necessary with mild heating) in CH_3CN and the solution dried with K_2CO_3. The solution was filtered and the desiccant washed with hot CH_3CN. After removal of the solvent a beige powder (450 mg, 0.96 mmol, 96%) was isolated. Crystals were obtained from a saturated CH_3CN solution. $C_{22}H_{32}N_{10}O_2$ (468.56)·$3H_2O$: calcd. C 50.56, H 7.33, N 26.80; found C 51.02, H 7.22, N 26.62. ^1H NMR (399.89 MHz, CD_2Cl_2, 295.3 K): δ = 6.74–6.69 (m, 4 H, $CH_{arom.}$), 4.80 (s, 4 H, CH), 2.88 (s, 12 H, CH_3), 2.74 (s, 12 H, CH_3) ppm. ^{13}C NMR (100.56 MHz, CD_2Cl_2, 295.5 K): δ = 158.68 (CO), 149.05 (CN_3), 141.31, 122.34, 122.82 ($C_{arom.}$), 74.84 (CH), 33.07, 30.03 (CH_3) ppm. MS (ESI, CH_3CN): *m/z* (%) = 469 (100) $[M]^+$. IR (CsI): $\tilde{\nu}$ = 2939 (w), 2880 (sh), 1700 (vs), 1636 (vs), 1581 (m), 1512 (s), 1475 (m), 1415 (m), 1373 (w), 1297 (w), 1232 (s), 1162 (w), 1104 (w), 1033 (vs), 879 (w), 854 (w), 781 (s), 694 (w), 579 (m) cm^{-1}. UV/Vis (CH_3CN, $c = 9.61\times10^{-5}$ mol L^{-1}): λ_{max} (ε, $L\,mol^{-1}\,cm^{-1}$) = 225 (2.31×10^4, with a shoulder at 234), 267 (0.94×10^4), 306 (0.65×10^4) nm. Crystal data for $C_{22}H_{32}N_{10}O_2$·$3H_2O$: $C_{22}H_{38}N_{10}O_5$, M_r = 522.62, $0.40\times0.40\times0.35$ mm^3, monoclinic, space group *C*2/*c*, *a* = 12.775(3) Å, *b* = 15.945(3) Å, *c* = 13.441(3) Å, β = 108.96(3)°, *V* = 2589.4(11) $Å^3$, *Z* = 4, $d_{calcd.}$ = 1.341 $Mg\,m^{-3}$, Mo-K_α radiation (graphite-monochromated, λ = 0.71073 Å), *T* = 100 K, θ_{range} 2.11 to 30.08°. Reflections measured: 13338, independent: 3781, R_{int} = 0.0347. Final *R* indices [$I>2\sigma(I)$]: R_1 = 0.0420, wR_2 = 0.1121.

Ligand 2: Bicyclic tetramethylbisurea (1.0 g, 5.03 mmol) was suspended in toluene (30 mL). After the dropwise addition of oxalyl chloride (5 mL, 57.3 mmol) by syringe, the reaction mixture was stirred at 80–90 °C for 20 h. After removal of the solvent under high vacuum the residue was washed 3–4 times with Et_2O, leaving a beige residue (865 mg), which consisted of ca. 30% activated and 70% deactivated bisurea; yield 1.15 mmol, 23%. ^1H NMR (200 MHz, $CDCl_3$): δ = 6.28 (s, 2 H, CH), 3.49 (s, 6 H, CH_3), 3.07 (s, 6 H, CH_3) ppm. The activated urea was dissolved in CH_3CN (12 mL), and triethylamine (0.5 mL, 3.6 mmol) and 1,2,4,5-tetraaminobenzene·4HCl (78 mg, 0.28 mmol) were added to the reaction mixture at a temperature of 0 °C. After 30 min, NaOH solution (0.58 mL, 25% in H_2O) was added, and the solvent was removed under high vacuum. The residue was suspended in H_2O and filtered. The solid collected was redissolved in CH_3OH, and the solvent was removed to yield a beige powder (129 mg, 0.15 mmol, 54%). Crystals were grown from a saturated CH_3CN solution. $C_{38}H_{58}N_{20}O_4$ (859.01)·$8H_2O$: calcd. C 45.50, H 7.44, N 27.93; found C 45.54, H 7.47, N 27.93. ^1H NMR (399.89 MHz, CD_2Cl_2, 295.4 K): δ = 6.16 (s, 2 H, $CH_{arom.}$), 4.78 (s, 8 H, CH), 2.88 (s, 24 H, CH_3), 2.78 (s, 24 H, CH_3) ppm. ^{13}C NMR (100.56 MHz, CD_2Cl_2, 295.0 K): δ = 158.70 (CO), 149.09 (CN_3), 134.76, 115.98, ($C_{arom.}$), 74.87 (CH), 33.26, 30.11 (CH_3) ppm. MS (FAB): *m/z* (%) = 859 (100) $[M]^+$. IR (CsI): $\tilde{\nu}$ = 2934 (m), 2884 (sh), 1692 (vs), 1634 (vs), 1510 (s), 1413 (s), 1371 (m), 1236 (s), 1164 (m), 1035 (vs), 904 (m), 787 (m), 755 (w), 669 (w), 662 (w), 579 (w) cm^{-1}. UV/Vis (CH_3CN, $c = 6.72\times10^{-5}$ mol L^{-1}): λ_{max} (ε, $L\,mol^{-1}\,cm^{-1}$) = 247 (3.37×10^4), 290 (0.94×10^4), 347 (1.22×10^4) nm. CV (CH_3CN, SCE, 50 mV s^{-1}): $E_{1/2}$ (**2**/**2**$^{2+}$) = –0.15 V. Crystal data for **2**·$4CH_3OH$·$2H_2O$: $C_{42}H_{76}N_{22}O_{10}$, M_r = 1049.25, $0.35\times0.35\times0.35$ mm^3, triclinic, space group $P\bar{1}$, *a* = 8.4840(17) Å, *b* = 9.3670(19) Å, *c* = 17.136(3) Å, α = 89.39(3)°, β = 88.21(3)°, γ = 72.65(3)°, *V* = 1299.2(5) $Å^3$, *Z* = 1, $d_{calcd.}$ = 1.341 $Mg\,m^{-3}$, Mo-K_α radiation (graphite-monochromated, λ = 0.71073 Å), *T* = 100 K, θ_{range} 2.28 to 30.07°. Reflections measured: 13894, independent: 7551, R_{int} = 0.0364. Final *R* indices [$I>2\sigma(I)$]: R_1 = 0.0542, wR_2 = 0.1324.

(1H$_2$)Cl$_2$: Bisguanidine **1** (62 mg, 0.13 mmol) was dissolved in CH_3OH (3 mL). A HCl (2 M, 0.2 mL, 0.4 mmol) solution in Et_2O was added dropwise by syringe, and the clear, colorless reaction mixture was stirred at room temp. for 30 min. The solvent was removed under high vacuum and the colorless residue washed three times with Et_2O; yield 61 mg (0.11 mmol, 87%). Crystals were grown from a saturated CH_3OH solution at –20 °C. $C_{22}H_{34}Cl_2N_{10}O_2$ (540.22)·H_2O: calcd. C 47.29, H 6.50, N 25.08; found C 47.06, H 6.52, N 24.89. ^1H NMR (399.89 MHz, CD_3OD, 295.1 K): δ = 7.50 (s, 4 H, $CH_{arom.}$), 5.43 (s, 4 H, CH), 2.98 (s, 12 H, CH_3), 2.95 (s, 12 H, CH_3) ppm. ^{13}C NMR (100.56 MHz, CD_3OD, 295.7 K): δ = 160.66 (CO or CN_3), 129.21 ($C_{arom.}$), 78.71 (CH), 34.36, 31.38 (CH_3) (low signal intensity due to low solubility) ppm.

^{1}H NMR (200 MHz, CD_3CN): δ = 12.01 (s, 2 H, NH), 7.43 (s, 4 H, $CH_{arom.}$), 5.25 (s, 4 H, CH), 3.03 (s, 12 H, CH_3), 2.96 (s, 12 H, CH_3) (low signal intensity due to low solubility) ppm. MS (ESI, CH_3OH): *m/z* (%) = 469 (100) $[M - H]^+$. IR (CsI): $\tilde{\nu}$ = 2942 (w), 2865 (sh), 1706 (vs), 1634 (vs), 1587 (vs), 1497 (s), 1419 (s), 1359 (m), 1235 (vs), 1159 (m), 1037 (vs), 956 (w), 896 (w), 789 (s), 694 (m), 580 (m) cm^{-1}. Crystal data for $(\mathbf{1H}_2)Cl_2 \cdot H_2O$, $C_{22}H_{36}Cl_2N_{10}O_3$, M_r = 559.51, 0.30 × 0.20 × 0.20 mm^3, monoclinic, space group $P2_1/n$, a = 12.606(3) Å, b = 12.844(3) Å, c = 16.472(3) Å, β = 94.92(3)°, V = 2657.2(9) Å^3, Z = 4, $d_{calcd.}$ = 1.399 $Mg\,m^{-3}$, Mo-K_α radiation (graphite-monochromated, λ = 0.71073 Å), T = 100 K, θ_{range} 2.01 to 30.04°. Reflections measured: 15139, independent: 7749, R_{int} = 0.0630. Final R indices [$I > 2\sigma(I)$]: R_1 = 0.0638, wR_2 = 0.1634.

$(2H_4)Cl_4$: Compound **2** (34 mg, 0.04 mmol) was dissolved in CH_3OH (5 mL). A HCl (2 M, 0.13 mL, 0.26 mmol) solution in Et_2O was added dropwise by syringe. The pale yellow solution was stirred at room temp. for 20 h. The solvent was removed under vacuum, and the colorless residue washed three times with CH_3CN/Et_2O; yield 22 mg (0.022 mmol, 55%). Colorless crystals (unfortunately not suitable for XRD analysis) were obtained from a concentrated CH_3OH solution at –20 °C. $C_{58}H_{62}Cl_4N_{20}O_4$ (1004.85)·$2H_2O$: calcd. C 43.85, H 6.39, N 26.91; found 44.04, H 6.41, N 26.06. ^{1}H NMR (399.89 MHz, CD_3OD, 294.9 K): δ = 7.52 (s, 2 H, $CH_{arom.}$), 5.45 (s, 8 H, CH), 3.09 (s, 24 H, CH_3), 3.03 (s, 24 H, CH_3) ppm. ^{13}C NMR (100.56 MHz, CD_3OD, 295.7 K): δ = 160.63 (CO or CN_3), 126.96 ($C_{arom.}$), 78.73 (CH), 34.80, 31.46 (CH_3) ppm. The NMR analysis was hampered due to low solubility. IR (CsI): $\tilde{\nu}$ = 2935 (w), 2878 (sh), 2808 (sh), 1710 (vs), 1624 (vs), 1579 (sh), 1516 (m), 1493 (m), 1460 (m), 1420 (s), 1354 (m), 1288 (m), 1234 (s), 1035 (vs), 895 (w), 812 (m), 787 (s), 754 (m), 693 (w), 578 (m) cm^{-1}. MS (ESI, CH_3OH): *m/z* (%) = 430 (100) $[M - 2H]^+$, 859 (80) $[M - 3H]^+$.

(1H)PF_6: Bisguanidine **1** (102 mg, 0.22 mmol) was dissolved in CH_3CN (6 mL). After the addition of NH_4PF_6 (36 mg, 0.22 mmol) the reaction mixture was stirred with heating to reflux for 30 min. The solvent was removed under high vacuum, and the colorless residue redissolved in CH_3CN. After addition of charcoal the solution was stirred for 30 min before the mixture was filtered through celite. The solvent was reomoved under vacuum, and the residue washed three times with Et_2O; yield 95 mg (0.15 mmol, 70%). ^{1}H NMR (399.89 MHz, CD_2Cl_2, 295.1 K): δ = 7.09–7.00 (m, 4 H, $CH_{arom.}$), 5.17 (s, 4 H, CH), 2.96 (s, 12 H, CH_3), 2.91 (s, 12 H, CH_3) ppm. ^{13}C NMR (100.56 MHz, CD_2Cl_2, 296.5 K): δ = 158.08 (CO), 154.90 (CN_3), 124.56, 123.04 ($C_{arom.}$), 76.23 (CH), 33.80, 30.20 (CH_3) ppm. ^{31}P NMR (161.89 MHz, CD_2Cl_2, 296.2 K): δ = –144.48 (septet) ppm. IR (CsI): $\tilde{\nu}$ = 2955 (w), 1714 (s), 1641 (s), 1592 (sh), 1500 (m), 1461 (sh), 1417 (m), 1367 (w), 1292 (sh), 1235 (s), 1158 (w), 1033 (s), 845 (vs), 784 (s), 703 (w), 559 (s) cm^{-1}.

(1H)BPh_4: (**1**H)PF_6 (85 mg, 0.138 mmol) was dissolved in acetone (3 mL) and CH_2Cl_2 (3 mL). $NaBPh_4$ (47 mg, 0.138 mmol) was added and the reaction mixture was stirred at room temp. for 1 h. After solvent removal under high vacuum, the colorless residue was washed three times with Et_2O. The product was recrystallized from CH_3OH; yield 97 mg (0.123 mmol, 89%) of crystalline product suitable for an XRD analysis. $C_{46}H_{53}BN_{10}O_2$ (788.44)·CH_3OH·CH_3CN: calcd. C 68.25, H 7.02, N 17.88; found C 68.49, H 6.74, N 17.57. ^{1}H NMR (399.89 MHz, CD_3CN, 294.9 K): δ = 7.28–7.25 (m, 8 H, $CH_{arom.}$), 7.10–7.08 (m, 2 H, $CH_{arom.}$), 7.07–7.04 (m, 2 H, $CH_{arom.}$), 6.99 (t, J = 7.49 Hz, 8 H, $CH_{arom.}$), 6.84 (t, J = 7.21 Hz, 4 H, BPh_4, $CH_{arom.}$), 5.04 (s, 4 H, CH), 2.88 (s, 12 H, CH_3), 2.77 (s, 12 H, CH_3) ppm. ^{13}C NMR (100.56 MHz, CD_3CN, 295.5 K): δ = 159.56 (CO), 136.63, 126.51, 126.11, 122.68 ($C_{arom.}$), 76.71 (CH), 33.68, 30.85 (CH_3) ppm. MS (ESI, CH_3CN/CH_3OH): *m/z* (%) = 469 (100) $[M]^+$. IR (CsI): $\tilde{\nu}$ = 3055 (w), 3000 (w), 2926 (w), 1713 (vs), 1635 (vs), 1588 (s), 1485 (s), 1415 (s), 1365 (w), 1232 (vs), 1158 (m), 1031 (vs), 887 (w), 848 (w), 774 (m), 740 (s), 708 (s), 612 (m), 578 (w) cm^{-1}. Crystal data for (**1H**)$BPh_4 \cdot 2CH_3OH \cdot CH_3CN$: $C_{50}H_{62}BN_{11}O_4$, M_r = 891.92, 0.30 × 0.25 × 0.25 mm^3, triclinic, space group $P\bar{1}$, a = 12.738(3) Å, b = 13.198(3) Å, c = 15.058(3) Å, α = 102.65(3), β = 92.18(3)°, γ = 94.02(3), V = 2460.3(8) Å^3, Z = 2, $d_{calcd.}$ = 1.204 $Mg\,m^{-3}$, Mo-K_α radiation (graphite-monochromated, λ = 0.71073 Å), T = 100 K, θ_{range} 2.42 to 29.00°. Reflections measured: 25156, independent: 12916, R_{int} = 0.0365. Final R indices [$I > 2\sigma(I)$]: R_1 = 0.0624, wR_2 = 0.1714.

$(2H_2)(PF_6)_2$: Compound **2** (53 mg 0.06 mmol) was dissolved in CH_3CN (10 mL), and NH_4PF_6 (23 mg, 0.14 mmol, 2.35 equiv.) was added. The reaction mixture was stirred at room temp. for 20 h. The solvent was removed under vacuum, and the pale yellow residue redissolved in CH_3CN. After addition of activated charcoal, the solution was stirred for 30 min before it was filtered through celite. The pale green residue obtained after removal of the solvent under vacuum was washed three times with Et_2O; yield 50 mg (0.043 mmol, 72%). $C_{38}H_{60}F_{12}N_{20}O_4P_2$ (1150.95)·$3H_2O$: calcd. C 37.88, H 5.52, N 23.25; found C 37.68, H 5.43, N 22.40. ^{1}H NMR (399.89 MHz, CD_3CN, 295.4 K): δ = 6.74 (br. s, 2 H, $CH_{arom.}$), 5.13 (s, 8 H, CH), 2.99 (s, 27 H, CH_3), 2.83 (s, 21 H, CH_3) ppm. ^{13}C NMR (100.56 MHz, CD_3CN, 296.5 K): δ = 159.60 (CN_3 or CO), 76.98 (CH), 33.82, 30.98 (CH_3) ppm. ^{31}P NMR (161.89 MHz, CD_3CN, 295.9 K): δ = –144.62 (septet) ppm. IR (CsI): 2943 (w), 2882 (sh), 1709 (s), 1690 (sh), 1625 (s), 1501 (m), 1453 (sh), 1416 (m), 1359 (w), 1285 (m), 1264 (m), 1234 (m), 1172 (w), 1030 (s), 845 (vs), 786 (s), 698 (w), 568 (m), 559 (s) cm^{-1}. MS (ESI, CH_3OH): *m/z* (%) = 430 (100) $[M]^+$, 1005 (62) $[M + PF_6]^+$, 859 (51) $[M - H]^+$.

$(2H_2)(BPh_4)_2$: (**2**H_2)$(PF_6)_2$ (40 mg, 0.035 mmol) was dissolved in CH_3OH (3 mL) and CH_2Cl_2 (3 mL). After addition of $NaBPh_4$ (26 mg, 0.076 mmol), the reaction mixture was heated to reflux for a short period of time and then stirred for 1 h at room temp. The solvent was removed under vacuum, the residue was recrystallized from CH_3OH, and washed three times with Et_2O; yield 38 mg (0.025 mmol, 72%). Crystals were grown by recrystallization from CH_3CN. ^{1}H NMR (399.89 MHz, CD_3CN, 293.8 K): δ = 7.27 (m, 16 H, BPh_4, $CH_{arom.}$), 6.99 (t, J = 7.40 Hz, 16 H, BPh_4, $CH_{arom.}$), 6.84 (t, J = 7.25 Hz, 8 H, BPh_4, $CH_{arom.}$), 6.65 (s, 2 H, $CH_{arom.}$), 5.06 (s, 8 H, CH), 2.88 (s, 24 H, CH_3), 2.80 (s, 24 H, CH_3) ppm. ^{13}C NMR (100.56 MHz, CD_3CN, 296.9 K): δ = 136.65, 126.49, 122.69 ($C_{arom.}$), 76.75 (CH), 33.74, 30.90 (CH_3) ppm. $C_{86}H_{100}B_2N_{20}O_4$ (1499.49)·$3H_2O$: calcd. C 66.49, H 6.88, N 18.03; found C 66.25, H 6.58, N 18.87. MS (ESI, CH_3OH): *m/z* (%) = 430 (93) $[M]^+$, 859 (100) $[M - H]^+$, 1179 (32) $[M + BPh_4]^+$. IR (CsI): $\tilde{\nu}$ = 3056 (w), 3037 (w), 2995 (w), 2934 (w), 1727 (sh), 1707 (vs), 1655 (sh), 1624 (vs), 1576 (w), 1506 (sh), 1494 (s), 1480 (sh), 1456 (m), 1450 (m), 1414 (s), 1358 (m), 1292 (m), 1267 (m), 1234 (s), 1177 (w), 1160 (w), 1127 (w), 1030 (vs), 967 (w), 903 (w), 889 (w), 849 (w), 789 (s), 740 (s), 708 (vs), 613 (s), 578 (m), 473 (w) cm^{-1}. Crystal data for (**2**H_2)$(BPh_4)_2 \cdot 8H_2O \cdot 6CH_3CN$: $C_{98}H_{134}B_2N_{26}O_{12}$, M_r = 1889.94, 0.30 × 0.30 × 0.25 mm^3, monoclinic, space group $P2_1/c$, a = 15.079(3) Å, b = 18.264(4) Å, c = 18.397(4) Å, β = 95.05(3)°, V = 5046.9(18) Å^3, Z = 2, $d_{calcd.}$ = 1.244 $Mg\,m^{-3}$, Mo-K_α radiation (graphite-monochromated, λ = 0.71073 Å), T = 100 K, θ_{range} 2.01 to 29.00°. Reflections measured: 27862, independent: 13351, R_{int} = 0.0488. Final R indices [$I > 2\sigma(I)$]: R_1 = 0.0629, wR_2 = 0.1513.

2(I$_3$)$_2$: I_2 (52 mg, 0.2 mmol) was added to a solution of **2** (86 mg, 0.1 mmol) in CH_3CN (5–10 mL). The reaction mixture adopted a green color, from which dark crystals precipitated. The precipitate was separated and washed several times with Et_2O; yield 71 mg (0.044 mmol, 63%). $C_{38}H_{58}I_6N_{20}O_4$ (1620.44): calcd. C 28.17, H 3.61, N 17.29; found C 27.83, H 3.64, N 16.76. ^{1}H NMR (399.89 MHz, CD_3CN, 295.2 K): δ = 5.34–5.26 (m, 2 H, $CH_{arom.}$, 8 H, CH), 2.94–2.87 (m, 48 H, CH_3) ppm. ^{13}C NMR (100.56 MHz, CD_3CN, 296.2 K): δ = 75.76, 76.12 (CH), 31.82 (CH_3) (low signal intensity due to low solubility) ppm. MS (ESI, CH_3OH): *m*/*z* (%) = 429 (100) $[M]^+$, 985 (42) $[MI]^+$. UV/Vis (CH_3CN, $c = 5.18\times10^{-5}$ mol L^{-1}): λ_{max} (ε, L mol^{-1} cm^{-1}) = 211 (1.85×10^4), 255 (1.80×10^4), 290 (4.60×10^4), 364 (2.37×10^4), 427 (2.48×10^4) nm. Crystal data for (**2**)(I$_3$)$_2$·2CH$_3$CN, $C_{42}H_{64}I_6N_{22}O_4$, M_r = 1702.56, $0.26\times0.20\times0.18$ mm^3, monoclinic, space group $P2_1/c$, a = 15.334(3) Å, b = 12.080(2) Å, c = 17.282(4) Å, β = 112.70(3)°, V = 2953.3(10) Å^3, Z = 2, $d_{calcd.}$ = 1.915 Mg m^{-3}, Mo-K_α radiation (graphite-monochromated, λ = 0.71073 Å), T = 100 K, θ_{range} 2.12 to 30.11°. Reflections measured: 16641, independent: 8647, R_{int} = 0.0329. Final R indices [$I>2\sigma(I)$]: R_1 = 0.0405, wR_2 = 0.0938.

[(1)PtCl(dmso)][PtCl$_3$(dmso)]: [$PtCl_2$(dmso)$_2$] (91 mg, 0.216 mmol) was added to a solution of **1** (50 mg, 0.107 mmol) in CH_2Cl_2 (10 mL). The reaction mixture was stirred for 20 h before the solvent was removed under high vacuum. The orange residue was dissolved in CH_3CN and filtered. The solvent was removed from the filtrate, and the residue washed several times with Et_2O. Diffusion of Et_2O into a solution of the product in CH_2Cl_2 led to an oily orange residue (yield 121 mg, 98%), which was again dissolved in CH_2Cl_2. Upon diffusion of Et_2O into this solution, orange crystals suitable for XRD analysis were obtained. $C_{26}H_{44}Cl_4N_{10}O_4Pt_2S_2$ (1156.79)·CH_2Cl_2: calcd. C 26.12, H 3.73, N 11.28; found C 25.81, H 4.11, N 11.47. ^{1}H NMR (399.89 MHz, CH_3CN, 295.0 K): δ = 6.65–6.62, 6.44–6.37 (m, 4 H, $CH_{arom.}$), 5.46, 5.20 (s, 4 H, CH), 3.43–2.93 [m, 12 H, (CH_3 in dmso), 24 H, CH_3] ppm. ^{13}C NMR (100.56 MHz, CH_3CN, 295.0 K): δ = 121.20 ($C_{arom.}$), 76.80, 76.76, 75.29 (CH), 46.07, 46.03, 43.90 [CH_3 in dmso], 33.29, 33.26, 33.11, 32.57, 31.71, 31.33, 31.29 (CH_3) ppm. MS (ESI, CH_3OH): *m*/*z* (%): 777 (100) $[M]^+$, 662 (7) $[(1)Pt]^+$, 698 (3) $[(1)PtCl]^+$. UV/Vis (CH_3CN, $c = 4.80\times10^{-5}$ mol L^{-1}): λ_{max} (ε, L mol^{-1} cm^{-1}) = 229 (3.90×10^4), 286 (1.14×10^4), 331 (0.45×10^4), 460 (0.12×10^4) nm. Crystal data for $C_{26}H_{44}Cl_4N_{10}O_4Pt_2S_2$: M_r = 1156.81, $0.20\times0.20\times0.18$ mm^3, triclinic, space group $P\bar{1}$, a = 9.0590(18) Å, b = 13.248(3) Å, c = 18.994(4) Å, α = 72.73(3)°, β = 78.22(3)°, γ = 87.22(3)°, V = 2130.8(9) Å^3, Z = 2, $d_{calcd.}$ = 1.803 Mg m^{-3}, Mo-K_α radiation (graphite-monochromated, λ = 0.71073 Å), T = 100 K, θ_{range} 2.29 to 26.75°. Reflections measured: 16050, independent: 8763, R_{int} = 0.0407. Final R indices [$I>2\sigma(I)$]: R_1 = 0.0904, wR_2 = 0.2317.

[(2){PtCl(dmso)}$_2$][PtCl$_3$(dmso)]$_2$: Compound **2** (49 mg, 0.057 mmol) and [$PtCl_2$(dmso)$_2$] (98 mg, 0.233 mmol, 4.09 equiv.) were dissolved in CH_2Cl_2 (10 mL), and the reaction mixture was stirred at room temp. for 20 h. A red solid was obtained upon removal of the solvent under vacuum, which was redissolved in CH_2Cl_2. Addition of Et_2O produced the red precipitate again. After removal of the solvent with the aid of a pipette, the solid was again first dissolved in CH_2Cl_2 and then precipitated by addition of Et_2O. After solvent removal (by pipette), the product was dissolved in CH_3CN and the solution filtered. The solvent was removed under vacuum to give a dark red powder; yield 86 mg (0.038 mmol, 67.5%). Thin red needle-shaped crystals were grown from CH_3CN solutions at –20 °C; however, structural analysis through XRD was impossible. $C_{46}H_{82}Cl_8N_{20}O_8Pt_4S_4$ (2235.47 g/mol): calcd. C 24.75, H 3.71, N 12.56; found C 24.64, H 3.93, N 12.42. ^{1}H NMR (600.13 MHz, CH_3CN, 295.0 K): δ = 6.09–5.02 (several multiplets, 2 H, $CH_{arom.}$, 8 H, CH), 3.27 (s, 12 H, CH_3 in $[PtCl_3(dmso)]^-$), 3.43–2.75 (several multiplets, 12 H, CH_3 in dmso, 48 H, CH_3) ppm. ^{13}C NMR (150.92 MHz, CH_3CN, 295.0 K): δ = 99.37, 99.13, 98.17 ($C_{arom.}$), 76.56, 74.83 (CH), 46.07, 45.85, 43.77 (CH_3 in dmso), 33.56, 33.42, 33.16, 32.99, 32.95, 32.92–32.78, 32.61, 31.91, 31.86, 31.77, 31.70, 31.67, 31.64, 31.64, 31.59, 31.25, 31.19, 30.70 (CH_3) (low signal intensity due to poor solubility) ppm. MS (ESI, CH_3OH): *m*/*z* (%): 737 (100) $[M]^+$, 584 (60) $[(2)HPt(dmso)Cl]^+$. IR (CsI): $\tilde{\nu}$ = 3006 (m), 2924 (m), 1717 (s), 1627 (sh), 1579 (s), 1544 (s), 1504 (m), 1449 (w), 1408 (m), 1354 (s), 1288 (m), 1231 (m), 1135 (s), 1025 (vs), 976 (w), 934 (w), 860 (s), 790 (s), 694 (w), 579 (m), 444 (m) cm^{-1}. UV/Vis (CH_3CN, $c = 2.34\times10^{-5}$ mol L^{-1}): λ_{max} (ε, L mol^{-1} cm^{-1}) = 228 (53704), 244 (48649), 302 (14606), 390 (7784), 492 (2016) nm.

[(2){PtCl(C_2H_4)}$_2$][PtCl$_3$(C_2H_4)]$_2$: Compound **2** (35 mg, 0.04 mmol) and [$PtCl(C_2H_4)(\mu\text{-}Cl)]_2$ (47 mg, 0.08 mmol) were dissolved in $CHCl_3$ (5 mL), and the reaction mixture was stirred at room temp. for 20 h. After removal of the solvent the solid red residue was washed several times with Et_2O; yield 63 mg (0.031 mmol, 77%). Pale red crystals were grown by diffusion of Et_2O into a solution of CH_2Cl_2. Crystals suitable for XRD were obtained from a $CDCl_3$ solution in an NMR tube. $C_{46}H_{74}Cl_8N_{20}O_4Pt_4$ (2035.17 g/mol): calcd. C 27.15, H 3.66, N 13.76; found C 26.94, H 3.73, N 13.39. ^{1}H NMR (399.89 MHz, CH_3CN, 294.1 K): δ = 5.97–5.92, 5.75–5.63, 5.57–5.33 (m, 2 H, $CH_{arom.}$, 8 H, CH), 4.30 (s, 8 H, $H_{ethylene}$ in $[PtCl_3(C_2H_4)]^-$), 3.77 (m, ^2JPt-H = 119.58 Hz, 8 H, $H_{ethylene}$ of the cation), 3.12–2.97 (m, 48 H, CH_3) ppm. ^{13}C NMR (100.56 MHz, CH_3CN, 295.0 K): δ = 75.42 (m, CH), 67.69 ($C_{ethylene}$ in $[PtCl_3(C_2H_4)]^-$), 31.82 (m, CH_3) (low signal intensity due to low solubility) ppm. IR: (CsI) $\tilde{\nu}$ = 3468 (w), 2964 (m), 2928 (sh), 1734 (s), 1728 (sh), 1707 (sh), 1576 (sh), 1561 (s), 1544 (s), 1499 (m), 1410 (m), 1353 (s), 1262 (m), 1218 (m), 1173 (w), 1094 (s), 1022 (vs), 853 (m), 796 (s), 695 (w), 579 (w) cm^{-1}. MS (ESI, CH_3OH): *m*/*z* (%) = 687 (100) $[M]^+$. UV/Vis (CH_3CN, $c = 2.34\times10^{-5}$ mol L^{-1}): λ_{max} (ε, L mol^{-1} cm^{-1}) = 243 (79833), 261 shoulder (56299), 288 (32963), 373 (31769), 485 (5213). Crystal data for $C_{54}H_{82}Cl_{32}N_{20}O_4Pt_4$: M_r = 2990.12, $0.40\times0.35\times0.35$ mm^3, triclinic, space group $P\bar{1}$, a = 11.627(2) Å, b = 12.641(3) Å, c = 17.571(4) Å, α = 106.46(3)°, β = 91.18(3)°, γ = 101.04(3)°, V = 2423.1(8) Å^3, Z = 1, $d_{calcd.}$ = 2.049 Mg m^{-3}, Mo-K_α radiation (graphite-monochromated, λ = 0.71073 Å), T = 100 K, θ_{range} 2.29 to 26.75°. Reflections measured: 16050, independent: 8763, R_{int} = 0.0407. Final R indices [$I>2\sigma(I)$]: R_1 = 0.0904, wR_2 = 0.2317.

[(1)NiCl$_2$]: [(dme)$NiCl_2$] (25 mg, 0.11 mmol) was suspended in CH_3CN (5 mL) and cooled to –40 °C. A solution of **1** (51 mg, 0.109 mmol) in CH_3CN (5 mL) was added dropwise. Then the reaction mixture was stirred for 2 h at –40 °C and 20 h at room temp. The green solution was filtered through Celite, and the solvent removed from the filtrate under vacuum. The green residue was washed three times with Et_2O; yield 50 mg (0.084 mmol, 77%). Green plate-like crystals suitable for an XRD analysis were grown by diffusion of Et_2O into a CH_2Cl_2 solution of the product. $3C_{22}H_{32}N_{10}Cl_2NiO_2$ (598.16)·$2CH_2Cl_2$: calcd. C 41.58, H 5.13, N 21.39; found C 41.87, H 5.58, N 21.03. IR (CsI): $\tilde{\nu}$ = 2960 (w), 2934 (w), 2886 (sh), 1720 (s), 1705 (sh), 1601 (s), 1563 (vs), 1525 (s), 1485 (s), 1448 (w), 1415 (s), 1362 (m), 1288 (m), 1270 (m), 1233 (m), 1091 (sh), 1028 (vs), 890 (m), 862 (w), 837 (m), 794 (s), 782 (s), 756 (m), 656 (w), 580 (w), 480 (w) cm^{-1}. UV/Vis (CH_2Cl_2, $c = 2.7\times10^{-5}$ mol L^{-1}): λ_{max} (ε, L mol^{-1} cm^{-1}) = 250 (18179), 288 (16051), 306 (13875), 439 (597), 513 (296), 577 (230), 699 (130) nm. Crystal data for [(**1**)$NiCl_2$]·CH_2Cl_2: $C_{23}H_{34}Cl_4N_{10}NiO_2$, M_r =

683.11, $0.35 \times 0.30 \times 0.15$ mm^3, orthorhombic, space group Fdd2, a = 16.698(3) Å, b = 64.216(13) Å, c = 11.458(2) Å, V = 12286(4) Å^3, Z = 16, $d_{calcd.}$ = 1.477 Mg m^{-3}, Mo-K_α radiation (graphite-monochromated, λ = 0.71073 Å), T = 100 K, θ_{range} 2.18 to 29.99°. Reflections measured: 8955, independent: 8762, R_{int} = 0.0346. Final R indices [$I > 2\sigma(I)$]: R_1 = 0.0461, wR_2 = 0.0937.

[(2)(NiCl$_2$)$_2$]: [(dme)NiCl$_2$] (46 mg, 0.2 mmol) and **2** (89 mg, 0.1 mmol) were dissolved in CH_3CN (10 mL) at –40 °C. The reaction mixture was stirred for 1.5 h at –40 °C and then at room temp. for 2 h. The brown solution was filtered through Celite, which was washed with CH_2Cl_2. The solvent was removed from the pink filtrate in vacuo. The dark pink residue was washed three times with Et_2O; yield 92 mg (0.082 mmol, 82%). Pink needles, which were unfortunately not suitable for XRD analysis, were obtained by diffusion of Et_2O into a solution of the product in CH_2Cl_2 at 3 °C. $C_{38}H_{58}Cl_4N_{20}Ni_2O_4$ (1118.20)·0.5CH_2Cl_2: calcd. C 39.84, H 5.12, N 24.14; found C 39.81, H 5.43, N 23.23. IR (CsI): $\tilde{\nu}$ = 2968 (sh), 2940 (w), 2879 (sh), 1712 (sh), 1576 (m), 1524 (m), 1493 (m), 1413 (m), 1360 (m), 1273 (m), 1227 (m), 1170 (w), 1090 (w), 1026 (vs), 973 (w), 923 (w), 857 (m), 819 (w), 791 (m), 726 (w), 579 (m), 468 (w) cm^{-1}. UV/Vis (CH_2Cl_2, $c = 4.34 \times 10^{-5}$ mol L^{-1}): λ_{max} (ε, L mol^{-1} cm^{-1}) = 252 (24889), 274 (27777), 317 (20429), 341 (19763), 466 (1196), 529 (1008), 591 (716), 702 (235) nm.

[(1)PdCl$_2$]: [PdCl$_2$(cod)] (22 mg, 0.077 mmol) and **1** (32 mg, 0.068 mmol) were dissolved in CH_2Cl_2 (10 mL). The blue-green solution was stirred at room temp. for 20 h and filtered through Celite. The solvent was removed under vacuum and the residue washed twice with petroleum ether 40–60 and Et_2O; yield 42 mg (0.065 mmol, 96%). Green needles suitable for XRD were obtained by diffusion of Et_2O into a CH_2Cl_2 solution of the product. $C_{22}H_{32}Cl_2N_{10}O_2Pd$ (642.89)·0.25CH_2Cl_2: calcd. C 40.06, H 4.91, N 21.00; found C 40.14, H 5.05, N 20.73. ^{1}H NMR (399.89 MHz, $CDCl_3$, 295.8 K): δ = 6.61 (dd, J = 5.76, 3.32 Hz, 2 H, $CH_{arom.}$), 6.38 (dd, J = 5.86, 3.40 Hz, 2 H, $CH_{arom.}$), 5.30 (4 H, CH), 3.27 (12 H, CH_3), 3.04 (12 H, CH_3) ppm. ^{13}C NMR (100.56 MHz, $CDCl_3$, 297.3 K): δ = 167.33 (CO), 158.04 (CN_3), 142.95, 120.21, 115.79 ($C_{arom.}$), 75.31 (CH), 34.41, 30.48 (CH_3) ppm. IR (CsI): $\tilde{\nu}$ = 2962 (w), 2932 (w), 2883 (sh), 1731 (sh), 1720 (vs), 1698 (sh), 1583 (sh), 1561 (vs), 1527 (s), 1491 (s), 1447 (w), 1407 (s), 1387 (w), 1351 (s), 1292 (sh), 1276 (m), 1236 (m), 1092 (sh), 1024 (vs), 887 (w), 851 (m), 831 (m), 789 (m), 785 (m), 752 (m), 656 (w), 576 (w), 542 (w), 480 (w) cm^{-1}. UV/Vis (CH_3CN, $c = 2.73 \times 10^{-5}$ mol L^{-1}): λ_{max} (ε, L mol^{-1} cm^{-1}) = 231 (38575), 299 (13028), 333 (6044), 425 (594), 605 (838) nm. Crystal data for [(**1**)PdCl$_2$]·2CH_2Cl_2: $C_{24}H_{36}Cl_6N_{10}O_2Pd$, M_r = 815.73, $0.35 \times 0.20 \times 0.15$ mm^3, monoclinic, space group $P2_1/c$, a = 12.544(3) Å, b = 23.560(5) Å, c = 11.841(2) Å, β = 107.74(3)°, V = 3333.1(12) Å^3, Z = 4, $d_{calcd.}$ = 1.626 Mg m^{-3}, Mo-K_α radiation (graphite-monochromated, λ = 0.71073 Å), T = 100 K, θ_{range} 2.24 to 30.12°. Reflections measured: 53827, independent: 9791, R_{int} = 0.0833. Final R indices [$I > 2\sigma(I)$]: R_1 = 0.0589, wR_2 = 0.1504.

[(1)Pd(η^3-C$_3$H$_5$)][PdCl$_2$(η^3-C$_3$H$_5$)]: [PdCl(η^3-C$_3$H$_5$)]$_2$ (35 mg, 0.096 mmol) and **1** (45 mg, 0.096 mmol) were dissolved in $CHCl_3$ (6 mL). The reaction mixture was stirred for 3 h (in a closed, elongated Schlenk tube) under reflux and at room temp. for a further hour. The yellow solution was filtered through Celite and the Celite was washed with CH_2Cl_2. The solvent was removed from the filtrate under vacuum. The yellow residue was washed three times with Et_2O; yield 57 mg (0.068 mmol, 71%). Yellow needle-shaped crystals were obtained by diffusion of Et_2O into a solution of the product in CH_2Cl_2. $C_{28}H_{42}Cl_2N_{10}O_2Pd_2$ (834.45): calcd. C 40.30, H 5.07, N 16.79; found C 40.06, H 5.20, N 16.29. ^{1}H NMR (399.89 MHz, $CDCl_3$, 296.5 K): δ = 6.74 (m, 2 H, $CH_{arom.}$) 6.60 (m, 2 H, $CH_{arom.}$), 5.95 (m, 1 H, CH_{allyl}), 5.61 (br. s, 4 H, CH), 5.37 (m, 1 H, CH_{allyl}), 3.98 (d, J = 6.56 Hz, 2 H, $CH_{2\ allyl}$), 3.80 (J = 6.37 Hz, 2 H, $CH_{2\ allyl}$), 3.15 (d, J = 12.02 Hz, 2 H, $CH_{2\ allyl}$), 3.04 (s, 12 H, CH_3), 3.02 (s, 12 H, CH_3), 2.91 (d, J = 12.11 Hz, 2 H, $CH_{2\ allyl}$) ppm. ^{13}C NMR (100.56 MHz, $CDCl_3$, 297.7 K): δ = 129.45, 128.44, 123.54, 121.34, ($C_{arom.}$), 109.88 (CH_{allyl}), 75.15 (CH), 61.40 ($CH_{2\ allyl}$), 34.17, 30.99 (CH_3) ppm. IR (CsI): $\tilde{\nu}$ = 3060 (w), 2952 (w), 2887 (sh), 1722 (s), 1581 (sh), 1549 (vs), 1489 (s), 1450 (w), 1410 (s), 1362 (m), 1295 (m), 1272 (m), 1233 (m), 1121 (w), 1026 (vs), 964 (w), 945 (w), 888 (m), 843 (m), 787 (m), 754 (s), 660 (w), 579 (m), 538 (w), 510 (w), 481 (w) cm^{-1}. MS (ESI, CH_2Cl_2): m/z (%): 615 (100) [(**1**)Pd(η^3-C$_3$H$_5$)]. UV/Vis (CH_2Cl_2, $c = 7.19 \times 10^{-5}$ mol L^{-1}): λ_{max} (ε, L mol^{-1} cm^{-1}) = 233 (37201), 293 (9864), 380 (1934) nm. Crystal data for [(**1**)Pd(C$_3$H$_5$)]-[PdCl$_2$(C$_3$H$_5$)]: $C_{28}H_{42}Cl_2N_{10}O_2Pd_2$, M_r = 834.42, $0.30 \times 0.15 \times 0.15$ mm^3, triclinic, space group $P\bar{1}$, a = 9.850(2) Å, b = 12.858(3) Å, c = 13.618(3) Å, α = 71.66(3)°, β = 83.67(3)°, γ = 88.36(3)°, V = 1627.2(6) Å^3, Z = 2, $d_{calcd.}$ = 1.703 Mg m^{-3}, Mo-K_α radiation (graphite-monochromated, λ = 0.71073 Å), T = 100 K, θ_{range} 2.48 to 33.00°. Reflections measured: 21275, independent: 12086, R_{int} = 0.0373. Final R indices [$I > 2\sigma(I)$]: R_1 = 0.0422, wR_2 = 0.0978.

[(2){Pd(η^3-C$_3$H$_5$)}$_2$][PdCl$_2$(η^3-C$_3$H$_5$)]$_2$: [PdCl(η^3-C$_3$H$_5$)]$_2$ (22 mg, 0.06 mmol) and **2** (26 mg, 0.03 mmol) were dissolved in $CHCl_3$ (6 mL). The reaction mixture was heated (in a closed, elongated Schlenk tube) to reflux for 3 h and stirred at room temp. for a further hour. The orange solution was filtered through Celite (which was washed subsequently with small amounts of CH_2Cl_2). The solvent was removed from the filtrate under vacuum and the residue washed three times with Et_2O; yield 30 mg (0.018 mmol, 63%). Crystals were obtained by diffusion of Et_2O into a solution of the product in CH_2Cl_2. Yellow needles suitable for XRD were obtained. $C_{50}H_{78}Cl_4N_{20}O_4Pd_4$ (1590.79)·2CH_2Cl_2: calcd. C 35.47, H 4.69, N 15.91; found C 36.00, H 4.90, N 15.82. ^{1}H NMR (399.89 MHz, $CDCl_3$, 296.4 K): δ = 6.35 (m, 2 H, $CH_{arom.}$, 2 H, CH); 6.09 (m, 4 H, CH), 5.87 (m, 2 H, CH), 5.50 (m, 2 H, CH_{allyl}), 5.34 (m, 2 H, CH_{allyl}), 3.98 (d, J = 6.63 Hz, 4 H, $CH_{2\ allyl}$), 3.30 (dd, J = 6.49, 3.69 Hz, 4 H, $CH_{2\ allyl}$), 3.18 (s, 6 H, CH_3), 3.06 (s, 6 H, CH_3), 3.04 (s, 6 H, CH_3), 3.03 (s, 6 H, CH_3), 3.01 (br. s, 12 H, CH_3), 2.95 (d, J = 12.31 Hz, 4 H, $CH_{2\ allyl}$), 2.90 (s, 6 H, CH_3), 2.86 (d, J = 11.88 Hz, 4 H, $CH_{2\ allyl}$), 2.79 (s, 6 H, CH_3) ppm. ^{13}C NMR (150.56 MHz, $CDCl_3$, 297.8 K): δ = 83.93, 75.47, 75.27, 74.90 (CH), 61.15 ($CH_{2\ allyl}$), 35.00, 34.19, 33.78, 32.99, 32.05, 31.31, 31.21, 30.49 (CH_3) ppm. IR (CsI): $\tilde{\nu}$ = 2938 (w), 2875 (sh), 1716 (s), 1553 (vs), 1522 (s), 1497 (s), 1458 (w), 1407 (s), 1360 (s), 1272 (m), 1224 (m), 1177 (w), 1128 (w), 1088 (w), 1022 (vs), 966 (w), 929 (w), 855 (m), 827 (w), 789 (s), 757 (w), 734 (w), 700 (w), 663 (w), 577 (m), 515 (w), 481 (w) cm^{-1}. MS (ESI, CH_2Cl_2): m/z (%): 1005 (100) [(**2**)Pd(C$_3$H$_5$)]$^+$, 859 (47) [**2**H]$^+$, 577 (15) [M]$^+$. UV/Vis (CH_2Cl_2, $c = 3.69 \times 10^{-5}$ mol L^{-1}): λ_{max} (ε, L mol^{-1} cm^{-1}) = 241 (35254), 285 (13745), 360 (8705), 425 (2864) nm. Crystal data for [(**2**){Pd(C$_3$H$_5$)}$_2$][PdCl$_2$(C$_3$H$_5$)]$_2$·2CH_2Cl_2: $C_{52}H_{82}Cl_8N_{20}O_4Pd_4$, M_r = 1760.58, $0.20 \times 0.10 \times 0.10$ mm^3, triclinic, space group $P\bar{1}$, a = 9.3720(19) Å, b = 13.259(3) Å, c = 14.360(3) Å, α = 107.66(3)°, β = 95.22(3)°, γ = 94.72(3)°, V = 1681.9(6) Å^3, Z = 1, $d_{calcd.}$ = 1.738 Mg m^{-3}, Mo-K_α radiation (graphite-monochromated, λ = 0.71073 Å), T = 100 K, θ_{range} 2.20 to 30.10°. Reflections measured: 17756, independent: 9809, R_{int} = 0.0482. Final R indices [$I > 2\sigma(I)$]: R_1 = 0.0458, wR_2 = 0.0986.

Catalytic Test Experiment: 3[(**1**)NiCl$_2$]·2CH_2Cl_2 (1.156 mg, 1.6×10^{-3} mmol) was suspended in toluene (5 mL). Polymethylaluminoxane (PMAO) (2.03 g, 2985 equiv., 7% solution in toluene)

was added, and the mixture stirred for 20 min. The mixture was transferred by syringe to a second Schlenk tube, which contained toluene (50 mL) and ethylene. Additional ethylene was passed over the stirring solution at room temp. After 38 min, Et_2OH/HCl (95:5, 50 mL) was added and the organic phase washed three times with H_2O/HCl. The organic phase was finally analysed with GC/MS.

X-ray Crystallographic Study: Crystals were taken directly out of the mother liquor, immersed in perfluorinated polyether oil, and fixed on a glass capillary. Measurements were made with a Nonius-Kappa CCD diffractometer with a low temperature unit using graphite-monochromated Mo-K_α radiation. The temperature was set to 100 K. The data collected were processed using the standard Nonius software.[41] All calculations were performed using the SHELXT-PLUS software package. Structures were solved by direct methods with the SHELXS-97 program and refined with the SHELXL-97 program.[42,43] Graphical handling of the structural data during solution and refinement was performed with XPMA.[44] Atomic coordinates and anisotropic thermal parameters of non-hydrogen atoms were refined by full-matrix least-squares calculations.

CCDC-795587 (for **1**), -795588 [for (**1**H)(BPh_4)], -795590 [for (**1**H_2)Cl_2], -824160 [for (**2**H_2)(BPh_4)$_2$], -795591 (for **2**), -795593 [for (**2**)(I_3)$_2$], -795592 [for {(**1**)PtCl(dmso)}{$PtCl_3$(dmso)}], -824158 [for ({**2**}{PtCl(C_2H_4)}$_2$){$PtCl_3$(C_2H_4)}$_2$], -824159 [for{(**1**)$NiCl_2$}], -824161 [for {(**1**)$PdCl_2$}], -824163 [for {(**1**)Pd(η^3-C_3H_5)}{$PdCl_2$(η^3-C_3H_5)}], and -824162 [for ({**2**}{Pd(η^3-C_3H_5)}$_2$){$PdCl_2$(C_3H_5)}$_2$] contain the supplementary crystallographic data for this paper. These data can be obtained free of charge from The Cambridge Crystallographic Data Centre via www.ccdc.cam.ac.uk/data_request/cif.

Supporting Information (see footnote on the first page of this article): Molecular structure and crystal data for the product of the reaction of tetramethylbisurea and oxalyl chloride at temperatures exceeding 100 °C, IR spectra, TGA curve for [(**2**){PtCl(C_2H_4)}$_2$]-[$PtCl_3$(C_2H_4)]$_2$, selected UV/Vis spectra.

Acknowledgments

Continued financial support from the Deutsche Forschungsgemeinschaft (DFG) is gratefully acknowledged.

[1] L. K. Johnson, C. M. Killian, M. Brookhart, *J. Am. Chem. Soc.* **1995**, *117*, 6414–6415.
[2] S. D. Ittel, S. Mecking, M. Brookhart, *Chem. Rev.* **2000**, *100*, 1169–1204.
[3] V. C. Gibson, C. Redshaw, G. A. Solan, *Chem. Rev.* **2007**, *107*, 1745–1776.
[4] a) F. T. Edelmann, *Adv. Organomet. Chem.* **2008**, *57*, 183–352; b) F. T. Edelmann, *Chem. Soc. Rev.* **2009**, *38*, 2253–2268.
[5] a) M. P. Coles, *Dalton Trans.* **2006**, 985–1001; b) M. P. Coles, *Chem. Commun.* **2009**, 3659–3676; c) M. P. Coles, P. J. Aragón-Sáez, S. H. Oakley, P. B. Hitchcock, M. G. Davidson, Z. B. Maksić, R. Vianello, I. Leito, I. Kaljurand, D. C. Apperley, *J. Am. Chem. Soc.* **2009**, *131*, 16858–16868.
[6] a) F. A. Cotton, J. H. Matonic, C. A. Murillo, *J. Am. Chem. Soc.* **1997**, *19*, 7889–7890; b) F. A. Cotton, L. M. Daniels, C. A. Murillo, D. J. Timmons, *Chem. Commun.* **1997**, 1449–1450; c) F. A. Cotton, N. E. Gruhn, J. Gu, P. Huang, D. L. Lichtenberger, C. A. Murillo, L. O. Van Dorn, C. C. Wilkinson, *Science* **2002**, *298*, 1971–1974; d) F. A. Cotton, J. Gu, C. A. Murillo, D. J. Timmons, *J. Am. Chem. Soc.* **1998**, *120*, 13280–13281; e) F. A. Cotton, J. P. Donahue, D. L. Lichtenberger, C. A. Murillo, D. Villagrán, *J. Am. Chem. Soc.* **2005**, *127*, 10808–10809; F. A. Cotton, N. S. Dalal, P. Huang, S. A. Ibragimov, C. A. Murillo, P. M. B. Piccoli, C. M. Ramsey, A. J. Schultz, X. Wang, Q. Zhao, *Inorg. Chem.* **2007**, *46*, 1718–1726.
[7] a) C. Würtele, E. Gaoutchenova, K. Harms, M. C. Holthausen, J. Sundermeyer, S. Schindler, *Angew. Chem.* **2006**, *118*, 3951–3954; *Angew. Chem. Int. Ed.* **2006**, *45*, 3867–3869; b) D. Maiti, D.-H. Lee, K. Gaoutchenova, C. Würtele, M. C. Hothausen, A. A. N. Sarjeant, J. Sundermeyer, S. Schindler, K. D. Karlin, *Angew. Chem.* **2007**, *120*, 88–91; *Angew. Chem. Int. Ed.* **2007**, *47*, 82–85; c) M. P. Lanci, V. V. Smirnov, C. J. Cramer, E. V. Gaoutchenova, J. Sundermeyer, J. P. Roth, *J. Am. Chem. Soc.* **2007**, *129*, 14697–14709.
[8] S. Herres-Pawlis, *Nachr. Chem.* **2009**, *57*, 20–23.
[9] a) S. Pohl, M. Harmjanz, J. Schneider, W. Saak, G. Henkel, *J. Chem. Soc., Dalton Trans.* **2000**, 3473–3479; b) D. Petrovic, L. M. R. Hill, P. G. Jones, W. B. Tolman, M. Tamm, *Dalton Trans.* **2008**, 887–894; c) S.-A. Filimon, C. G. Hrib, S. Randoll, I. Neda, P. G. Jones, M. Tamm, *Z. Anorg. Allg. Chem.* **2010**, *636*, 691–699.
[10] a) C. J. Carmalt, A. C. Newport, S. A. O'Neill, I. P. Parkin, A. J. P. White, D. J. Williams, *Inorg. Chem.* **2005**, *44*, 615–619; b) D. Rische, H. Parala, E. Gemel, M. Winter, R. A. Fischer, *Chem. Mater.* **2006**, *18*, 6075–6082; c) A. P. Milanov, R. Bhakta, A. Baunemann, H.-W. Becker, R. Thomas, P. Ehrhart, M. Winter, A. Devi, *Inorg. Chem.* **2006**, *45*, 11008–11018; d) J. P. Coyle, W. H. Monillas, G. P. A. Yap, S. T. Barry, *Inorg. Chem.* **2008**, *47*, 683–689; e) A. Baunemann, D. Bekermann, T. B. Thiede, H. Parala, M. Winter, C. Gemel, R. A. Fischer, *Dalton Trans.* **2008**, *28*, 3715–3722; f) A. P. Milanov, T. B. Thiede, A. Devi, R. A. Fischer, *J. Am. Chem. Soc.* **2009**, *131*, 17062–17063; g) S. E. Potts, C. J. Carmalt, C. S. Blackman, F. Abou-Chahine, D. Pugh, H. O. Davies, *Organometallics* **2009**, *28*, 1838–1844; h) A. P. Milanov, T. Toader, H. Parala, D. Barreca, G. A. Davide, C. Bock, H.-W. Becker, D. K. Ngwashi, R. Cross, S. Paul, U. Kunze, R. A. Fischer, A. Devi, *Chem. Mater.* **2009**, *21*, 5443–5455; i) T. Chen, W. Hunks, P. S. Chen, C. Xu, A. G. Di Pasquale, A. L. Rheingold, *Organometallics* **2010**, *29*, 501–504; j) A. P. Milanov, K. Xu, A. Laha, E. Bugiel, R. Ranjith, D. Schwendt, H. J. Osten, H. Parala, R. A. Fischer, A. Devi, *J. Am. Chem. Soc.* **2010**, *132*, 36–37.
[11] a) U. Wild, P. Roquette, E. Kaifer, J. Mautz, H. Wadepohl, H.-J. Himmel, *Eur. J. Inorg. Chem.* **2008**, 1248–1257; b) U. Wild, O. Hübner, A. Maronna, M. Enders, E. Kaifer, H. Wadepohl, H.-J. Himmel, *Eur. J. Inorg. Chem.* **2008**, 4440–4447; c) D. Domide, C. Neuhäuser, E. Kaifer, H. Wadepohl, H.-J. Himmel, *Eur. J. Inorg. Chem.* **2009**, 2170–2178; d) M. Reinmuth, U. Wild, E. Kaifer, M. Enders, H. Wadepohl, H.-J. Himmel, *Eur. J. Inorg. Chem.* **2009**, 4795–4808.
[12] M. Kawahata, K. Yamaguchi, T. Ho, T. Ishikawa, *Acta Crystallogr., Sect. E* **2006**, *62*, o3301–o3302.
[13] A. Peters, U. Wild, O. Hübner, E. Kaifer, H.-J. Himmel, *Chem. Eur. J.* **2008**, *14*, 7813–7821.
[14] T. Isobe, K. Fukuda, T. Ishikawa, *J. Org. Chem.* **2000**, *65*, 7770–7773.
[15] P. Roquette, C. König, O. Hübner, A. Wagner, E. Kaifer, M. Enders, H.-J. Himmel, *Eur. J. Inorg. Chem.* **2010**, 4770–4782.
[16] P. Roquette, A. Maronna, A. Peters, E. Kaifer, H.-J. Himmel, C. Hauf, V. Herz, E.-W. Scheidt, W. Scherer, *Chem. Eur. J.* **2010**, *16*, 1336–1350.
[17] P. Roquette, A. Maronna, M. Reinmuth, E. Kaifer, M. Enders, H.-J. Himmel, *Inorg. Chem.* **2011**, *50*, 1942–1955.
[18] A. Peters, E. Kaifer, H.-J. Himmel, *Eur. J. Org. Chem.* **2008**, 5907–5914.
[19] A. Peters, C. Trumm, M. Reinmuth, D. Emeljanenko, E. Kaifer, H.-J. Himmel, *Eur. J. Inorg. Chem.* **2009**, 3791–3800.
[20] D. Emeljanenko, A. Peters, N. Wagner, J. Beck, E. Kaifer, H.-J. Himmel, *Eur. J. Inorg. Chem.* **2010**, 1839–1846.
[21] V. Vitske, C. König, E. Kaifer, O. Hübner, H.-J. Himmel, *Eur. J. Inorg. Chem.* **2010**, 115–126.

[22] C. Trumm, O. Hübner, E. Kaifer, H.-J. Himmel, *Eur. J. Inorg. Chem.* **2010**, 3102–3108.
[23] A. Maronna, E. Bindewald, E. Kaifer, H. Wadepohl, H.-J. Himmel, *Eur. J. Inorg. Chem.* **2011**, 1302–1314.
[24] D. Emeljanenko, A. Peters, V. Vitske, E. Kaifer, H.-J. Himmel, *Eur. J. Inorg. Chem.* **2010**, 4783–4789.
[25] W. A. Freeman, W. L. Mock, N.-Y. Shih, *J. Am. Chem. Soc.* **1981**, *103*, 7367–7368.
[26] R. Wyler, J. de Mendoza, J. Rebek Jr., *Angew. Chem.* **1993**, *105*, 1820–1821; *Angew. Chem. Int. Ed. Engl.* **1993**, *32*, 1699–1701.
[27] J. Kang, J. Rebek Jr., *Nature* **1997**, *385*, 50–52.
[28] A. E. Rowan, J. A. A. W. Elemans, R. J. M. Nolte, *Acc. Chem. Res.* **1999**, *32*, 995–1006.
[29] F. Hof, S. L. Craig, C. Nuckolls, J. Rebek Jr., *Angew. Chem.* **2002**, *114*, 1556–1578; *Angew. Chem. Int. Ed.* **2002**, *41*, 1488–1508.
[30] For some representative recent studies, see: a) S.-Y. Kim, I.-S. Jung, E. Lee, J. Kim, S. Sakamoto, K. Yamaguchi, K. Kim, *Angew. Chem.* **2001**, *113*, 4363–4365; *Angew. Chem. Int. Ed.* **2001**, *40*, 2119–2121; b) W.-H. Huang, P. Y. Zavalij, L. Isaacs, *Angew. Chem.* **2007**, *119*, 7479–7490; *Angew. Chem. Int. Ed.* **2007**, *46*, 7425–7427; c) W.-H. Huang, P. Y. Zavalij, L. Isaacs, *J. Am. Chem. Soc.* **2008**, *130*, 8446–8454; d) Y. H. Ko, H. Kim, Y. Kim, K. Kim, *Angew. Chem.* **2008**, *120*, 4014–4017; *Angew. Chem. Int. Ed.* **2008**, *47*, 4106–4109; e) Y. Kim, H. Kim, Y. Hoko, N. Selvapalam, M. V. Rekharsky, Y. Inoue, K. Kim, *Chem. Eur. J.* **2009**, *15*, 6143–6151; f) J. Svec, M. Necas, V. Sindelar, *Angew. Chem.* **2010**, *122*, 2428–2431; *Angew. Chem. Int. Ed.* **2010**, *49*, 2378–2381.
[31] J. Nematollahi, R. Ketcham, *J. Org. Chem.* **1963**, *28*, 2378–2380.
[32] H. Petersen, *Synthesis* **1973**, 243–292.
[33] W. M. Koppes, M. Chaykovsky, H. G. Adolph, R. Gilardi, C. George, *J. Org. Chem.* **1987**, *52*, 1113–1119.
[34] M. O. Dekaprilevich, L. I. Suvorova, L. I. Khmelnitskii, *Acta Crystallogr., Sect. C* **1994**, *50*, 2056–2058.
[35] V. Raab, E. Gauchenova, A. Merkoulov, K. Harms, J. Sundermeyer, Z. B. Maksić, *J. Am. Chem. Soc.* **2005**, *127*, 15738–15743.
[36] V. Vitske, P. Roquette, S. Leingang, C. Adam, E. Kaifer, H. Wadepohl, H.-J. Himmel, *Eur. J. Inorg. Chem.* **2011**, 1593–1604.
[37] H. Isci, W. R. Mason, *Inorg. Chem.* **1985**, *24*, 271–274.
[38] Ligand geometry seems to play a minor role, as DFT calculations (where available) found energy minima with smaller Cl–Ni–Cl angles than determined experimentally.
[39] For recent structurally characterized examples, see, for example those with N-heterocyclic carbene ligands: a) A. T. Normand, A. Stasch, L.-L. Ooi, K. J. Cavell, *Organometallics* **2008**, *27*, 6507–6520; b) A. R. Chianese, P. T. Bremer, C. Wong, R. J. Reynes, *Organometallics* **2009**, *28*, 5244–5252.
[40] K. J. Cavell, D. S. McGuinness, *Coord. Chem. Rev.* **2004**, *248*, 671–679.
[41] DENZO-SMN, Data processing software, Nonius, **1998**; http://www.nonius.com.
[42] a) G. M. Sheldrick, *SHELXS-97*, *Program for Crystal Structure Solution*, University of Göttingen, **1997**; http://shelx.uni-ac.gwdg.de/SHELX/index.html; b) G. M. Sheldrick, *SHELXL-97*, *Program for Crystal Structure Refinement*, University of Göttingen, **1997**; http://shelx.uni-ac.gwdg.de/SHELX/index.html.
[43] *International Tables for X-ray Crystallography*, Vol. 4, Kynoch Press, Birmingham, U. K., **1974**.
[44] L. Zsolnai, G. Huttner, *XPMA*, University of Heidelberg, **1994**; http://www.uni-heidelberg.de/institute/fak12/AC/huttner/software/software.html.

Received: May 9, 2011
Published Online: August 16, 2011

